

**FIELD STUDY OF POTENTIAL POLLUTANT
MOVEMENT IN THE ENVIRONMENT**

Final Report

of

Project Number 55-61017

February 1, 1988

Funded By

TEXAS WATER DEVELOPMENT BOARD

By

C. B. Fedler

M. J. Dvoracek

K. A. Rainwater

R. H. Ramsey

TEXAS TECH UNIVERSITY

**FIELD STUDY OF POTENTIAL POLLUTANT
MOVEMENT IN THE ENVIRONMENT**

Final Report

of

Project Number 55-61017

February 1, 1988

Funded By

TEXAS WATER DEVELOPMENT BOARD

By

C. B. Fedler

M. J. Dvoracek

K. A. Rainwater

R. H. Ramsey

TEXAS TECH UNIVERSITY

**FIELD STUDY OF POTENTIAL POLLUTANT
MOVEMENT IN THE ENVIRONMENT**

TABLE OF CONTENTS

INTRODUCTION	1
BACKGROUND	1
OBJECTIVES	2
Task 1	2
Task 2	2
Task 3	2
DEVELOPMENT AND PROCEDURES	3
EROSION CHARACTERISTICS	3
Wind Erosion Model	3
Laboratory Tests	5
Field Sampling	5
UNSATURATED FLOW MODEL	5
Theoretical Development	5
Numerical Solution Procedure	9
GROUNDWATER TRACER TEST	9
Field Layout Design	9
Well Construction and Installation	10
Tracer Injection	15
Groundwater Sampling	17
Sample Analysis	17
Modeling Field Tracer Movement	17
THE USGS-2D MODEL	18
RESULTS AND DISCUSSION	20
EROSION CHARACTERISTICS	20
Wind Erosion Model	20
Field Deposits	22
2-D UNSATURATED FLOW MODEL	23
Vertical Solute Movement Simulation	23
GROUNDWATER TRACER TEST	25
Tracer Test Results	25
Model Setup	29
Model Results	31
Discussion of Modeling Efforts	42
CONCLUSIONS AND RECOMMENDATIONS	42
REFERENCES	45

APPENDIX A	47
APPENDIX B	69
APPENDIX C	73
APPENDIX D	76

LIST OF FIGURES

<u>Figure</u>	<u>Title</u>	<u>Page</u>
1	Effects of wind and water erosion on soil and possibly chemical deposition.	4
2	Site location for field samples of possible chemical movement.	6
3	Initial and boundary conditions for the flow equation and solute transport equation.	8
4	Location of well field in relation to area landmarks.	11
5	Layout of wells used in field study.	12
6	Estimated geological formation profile for line from Well A to Well L.	13
7	Estimated geological formation profile for line from Well C to Well E.	14
8	Equipment used during tracer injection.	16
9	The effects of wind erosion on a bare field with ridges.	21
10	Simulated concentration contours from the continuous tracer application to unsaturated soil.	24
11	Bromide concentration histories for Wells A through K arranged as in the field.	27
12	Transmissivity map and model grid used in the USGS-2D saturated flow model.	30
13	Bromide concentration history for actual and simulated data for Well D.	34
14	Bromide concentration history for actual and simulated data for Well E.	35
15	Bromide concentration history for actual and simulated data for Well G.	36
16	Bromide concentration history for actual and simulated data for Well H.	37
17	Bromide concentration contours for actual and simulated data for day 50 following tracer injection.	38

18	Bromide concentration contours for actual and simulated data for day 75 following tracer injection.	39
19	Bromide concentration contours for actual and simulated data for day 100 following tracer injection.	40
20	Bromide concentration contours for actual and simulated data for day 185 following tracer injection.	41

LIST OF TABLES

<u>Table</u>	<u>Title</u>	<u>Page</u>
1	Measured depths to water table from surface in test wells during study period.	28
2	Average and simulated water table elevations.	33

FIELD STUDY OF POTENTIAL POLLUTANT MOVEMENT IN THE ENVIRONMENT

INTRODUCTION

BACKGROUND

There is a general fear that exists today concerning the pollution of the nation's groundwater supply. This fear is justifiable when one considers that over 50 percent of the drinking water in the United States is from groundwater. More importantly, approximately 85 percent of the nation's rural population obtains their drinking water from groundwater. Adding to the groundwater demand, many municipal water supplies generate a portion of their flow from groundwater. Therefore, if a groundwater supply becomes polluted, the effect becomes widespread in terms of a health hazard.

The demand on our nation's groundwater supply extends beyond that used for drinking water. Much of the food crop produced in the United States utilizes groundwater as its primary source of irrigation water. The demand for irrigation is enormous; for example in Texas alone, over 7 million acres of cropland are irrigated for both food and fiber crops. On the national scale, over 50 million acres of land is irrigated (CAST, 1985). It follows that given a source of pollution in groundwater, the pollutant may eventually enter the natural food chain, thus affecting several millions of people in the long term.

Much of the blame for groundwater pollution is addressed as a non-point source. Generally, agriculture has been identified as the primary non-point source due to the large amounts of chemicals used in crop production. In order to maintain the present quality of life, pesticides of one kind or another will continue to be used by the producer. Pesticide application has allowed producers to grow a maximum quantity of material per unit area. It is estimated that over one billion pounds of pesticides are used in the U.S. with 68 percent of that applied to agricultural lands for crop production (Cheng and Koskinen, 1986).

One approach introduced to reduce the dependency on chemicals for pest control is integrated pest management (IPM). The IPM is a management program developed to allow a producer the same quality of pest control through tillage practices, scheduling and a reduced amount of pesticide. It is apparent that not all pesticide applications can be discontinued, but a substantial reduction in the volume used can be made.

Another alternative to reducing the persistence of a pesticide is the development of more biodegradable products. Many of the insecticides used today are degradable either biologically or photosynthetically. The more persistent insecticides are the water soluble and organochlorine types (Wauchope, 1978). In general, most pesticides presently used are synthetic organics. As a result, volatilization and decomposition occur within a short time, thus rendering the pesticide non-toxic. Of the more than 1000 pesticides registered with the EPA, approximately 50 have been identified as having the potential of reaching the groundwater only if conditions are favorable to downward movement (CAST, 1985).

After identification of the pesticides capable of entering the groundwater, the next problem is to determine the transport mechanism(s) that dominate(s) movement. The most direct pathway would be through a well that penetrates the aquifer. Even though this appears obvious, measures taken to assure that this direct pathway is blocked are not always practiced.

Once a contaminant enters a groundwater source, the inherent transport mechanism of the aquifer may move the contaminant to sectors used for drinking water purposes. Full understanding of the transport mechanisms are still being investigated, primarily in the laboratory.

OBJECTIVES

The primary objective of this research project was to conduct a field study of the potential movement of a pollutant in a groundwater in the Texas High Plains. Since this was a field study of an aquifer used by area residents, the test was restricted to a conservative solute. It was determined that insufficient insurance could be obtained to utilize a "hot" solute and guarantee recovery of the total amount of chemical injected into the aquifer. To determine the chemical movement in the soil profile and attempt to understand the interactions in the overall system, the following tasks were performed.

Task 1

Select several known erosion deposit areas from local fields known to have had a pesticide applied. Sample the erosion deposits from these fields to provide knowledge of the quantities of chemical movement due to erosion mechanisms.

Task 2

The second task was to examine the potential movement of a chemical attached to soil particles where erosion by wind is the primary transport mechanism.

Task 3

To use the information obtained from the first two tasks to develop an understanding of the overall picture of non-point source pollutants and groundwater, a computer simulation process using the USGS-2D model was performed. Vertical movement of a chemical is less understood and only a few site specific models exist so an unsaturated soil profile solute movement model was developed and used in this study.

DEVELOPMENT AND PROCEDURES

EROSION CHARACTERISTICS

Wind Erosion Model

A non-point source pollutant is one spread over a large area that eventually reaches a point in a water supply where the concentration exceeds the damage threshold for plant, animal, or human life. This occurrence of a pollutant means the non-point source pollutant was converted to a point source by some mechanism. The primary mechanism for this conversion could be soil erosion, caused by either wind or water.

In the United States, several million tons of soil are lost annually due to erosion. Most of this erosion occurs on agricultural lands where many different types of pesticides have been applied by the producer for pest management. Since many pesticides attach to soil particles, it is obvious that these pesticides can be transported to another location (Nicholson et al., 1964). Typically, erosion deposits are found in low-lying areas yet, obstructions such as fences, etc. can cause deposits from wind. If soil particles with an adsorbed pesticide are transported to these areas by erosion, the concentration of the pesticide would be higher than that found in the application area, thereby creating a "hot spot". Pesticides in the deposition area will either degrade in-situ or be transported via infiltration into the subsurface zone. When sufficient water is available, such as when ponding occurs in low lying deposit areas, the pesticide is in a favorable situation to be transported to the groundwater.

To assist the scientist in estimating the potential risk of pesticides from non-point sources in the environment, several surface-transport models have been developed (Mulkey et al., 1986). Generally, these models use erosion by water as the mechanism by which the soil and/or pesticide is transported. Unfortunately, another erosion transport mechanism does exist--wind.

Since the effects of water erosion on the transport of agricultural chemicals has been studied extensively (Leonard et al., 1979 and Zison, 1980), laboratory testing of chemical transport was restricted to possible movement caused by wind (Figure 1). The wind erosion model used in this study, developed by Gregory and Borrelli (1986), is made up of several submodels. Soil detachment potential, length of field, surface cover, and the wind velocity profile were used to derive the model. In summary, the primary model to describe the rate of soil movement for a specific length of field unprotected surface is:

$$X = C(SU_*^2 - U_{*t}^2) U_* (1 - e^{-0.000169A_a IL_f}) \quad [1]$$

where

X = rate of soil movement at length L_f (M/LT)

$C(SU_*^2 - U_{*t}^2)U_*$ = maximum rate of soil movement ($L = \infty$) which occurs when surface is covered with fine non-cohesive materials



Figure 1. Effects of wind and water erosion on soil and possibly chemical deposition.

- C = a constant which depends on width sampled and units used for U_* (MT^2/L^4)
 L_f = length of unprotected field in the direction of wind movement (L)
 A_a = abrasion adjustment term
 I = soil erodibility factor
 U_* = shear velocity (L/T)
 S = surface cover factor, and
 U_{*t} = threshold shear velocity (L/T).

Laboratory Tests

Preliminary wind tunnel tests using a constant wind velocity of 17.9 MPH were performed for the purpose of measuring the quantity of tracer attached to soil particles that moves with those particles under windy conditions. Using fine and medium size soil particles (≤ 0.1 mm), the tests were run in a wind tunnel to simulate the movement of approximately 10 tons/ac, or a soil layer that is approximately the thickness of a dime. Phosphorous was used as the tracer since it is non-volatile under the test conditions.

The soil was placed inside the wind tunnel, then treated with a mixture of potassium phosphate. The potassium phosphate was mixed into the soil surface to simulate actual field conditions. Two test conditions were examined as worst-case scenarios. The first was bare soil with little or no surface roughness while the second was bare soil with slight surface roughness due to clods, which were added to the surface.

Field Sampling

Soil samples were collected from selected field sites where erosion had occurred. All conditions were controlled by nature for the purpose of testing actual field conditions. The chemical used as the target chemical in this segment of the study was trifluralin (Treflan) applied at a rate of 1 qt/ac and incorporated into the soil surface. Treflan was selected because it is a widely used herbicide in the Texas High Plains and therefore should be present in the sediment deposits.

Figure 2 shows the layout of the area in which three sites were chosen. The first location, labeled A1 and A2 (duplicate sampling), was a site where water erosion had transported soil across the field with deposition at the field's low end. The second site, labeled B1 and B2, was located in a field where large amounts of soil was eroded and deposited, not only at the lower end of the field, but also across the road in a ditch. The third location (C1 and C2) was one in which little erosion other than wind should have occurred since the land was terraced to control water movement.

UNSATURATED FLOW MODEL

Theoretical Development

Based on the principle of mass balance and using the equation of continuity, a partial differential equation for unsaturated flow was developed

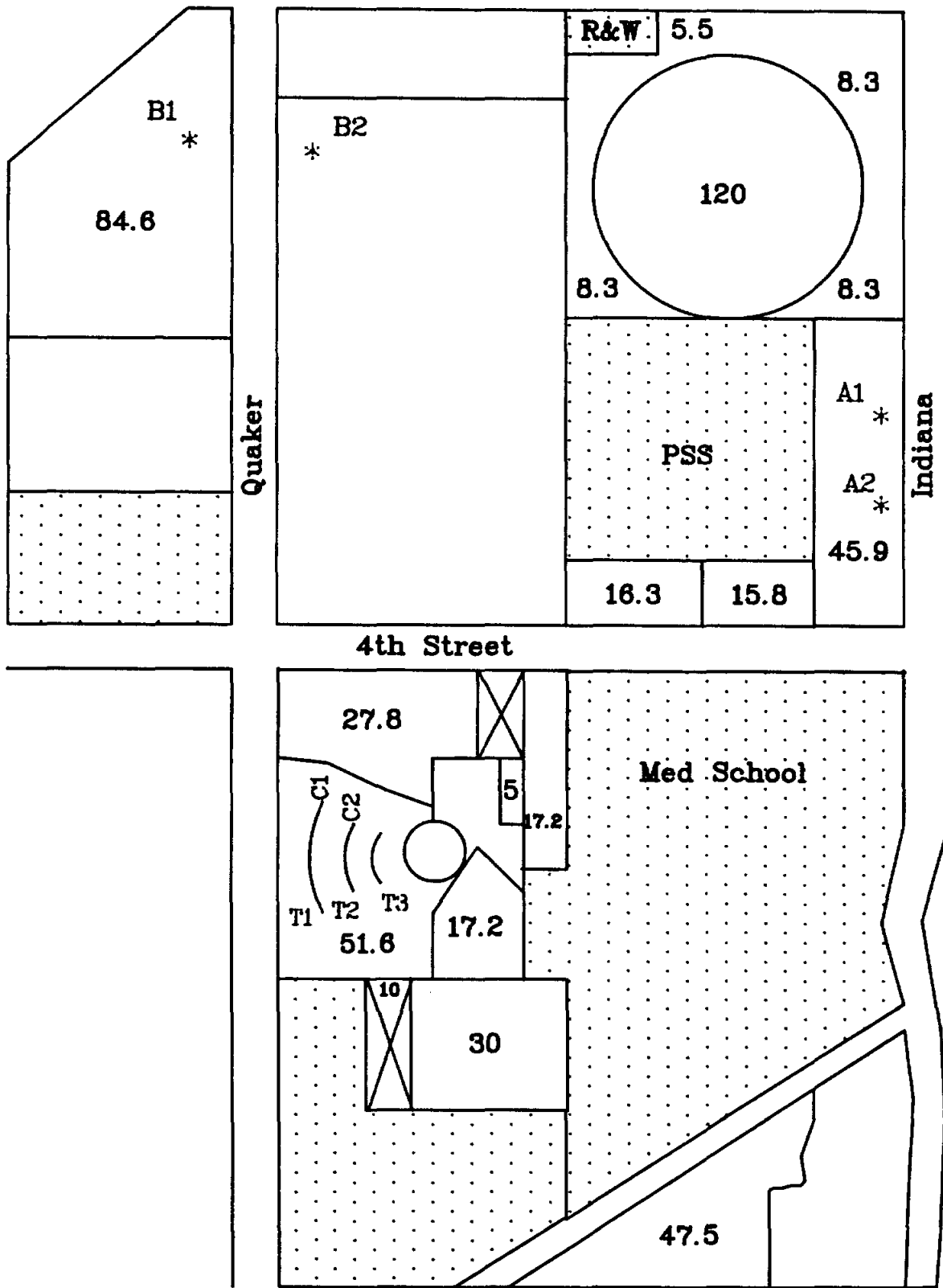


Figure 2. Site location for field samples of possible chemical movement.

similar to that developed by Hillel (1980). Using an elemental control volume as shown in Figure 3, the basic equation can be expressed as:

$$\text{mass in} - \text{mass out} = (\text{mass})/\partial t \quad [2]$$

The mass flow rate for Equation [2] is equal to the mass density of the liquid times the volumetric flow rate through the porous media. By continuity, the flow rate equals the velocity flux (q) times the area of flow (A). This results in a mass flow so that:

$$\text{mass in} = \rho q A_x - \frac{\partial (\rho q A_x)}{\partial x} \frac{dx}{2} \quad [3]$$

$$\text{mass out} = \rho q A + \frac{\partial (\rho q A_x)}{\partial x} \frac{dx}{2} \quad [4]$$

where x represents the flow direction and can be represented as y or z for the other two possible flow directions.

The net change in mass flow is the sum of the mass flow in all directions. By substituting the elemental lengths for area and assuming isothermal flow conditions, the flow equation in the x and z directions becomes:

$$\frac{\partial (q_x)}{\partial x} - \frac{\partial (q_z)}{\partial z} = \frac{\partial \theta}{\partial t} \quad [5]$$

Using Darcy's Law ($q = -k(dh/dl)$), the final equation for flow through unsaturated porous media is:

$$- \frac{\partial}{\partial x} \left[-k \frac{\partial (\psi+z)}{\partial x} \right] - \frac{\partial}{\partial z} \left[-k \frac{\partial (\psi+z)}{\partial z} \right] = \frac{\partial \theta}{\partial t} \quad [6]$$

where k = hydraulic conductivity of the soil (L/T)
 θ = volumetric soil moisture content (M/L³)
 z = depth of soil (positive downward) L
 ψ = capillary pressure head L
 t = time T

Equation [6] represents the flow of a liquid through the porous media, therefore, the following basic equation was used to represent the change in solute concentration over time.

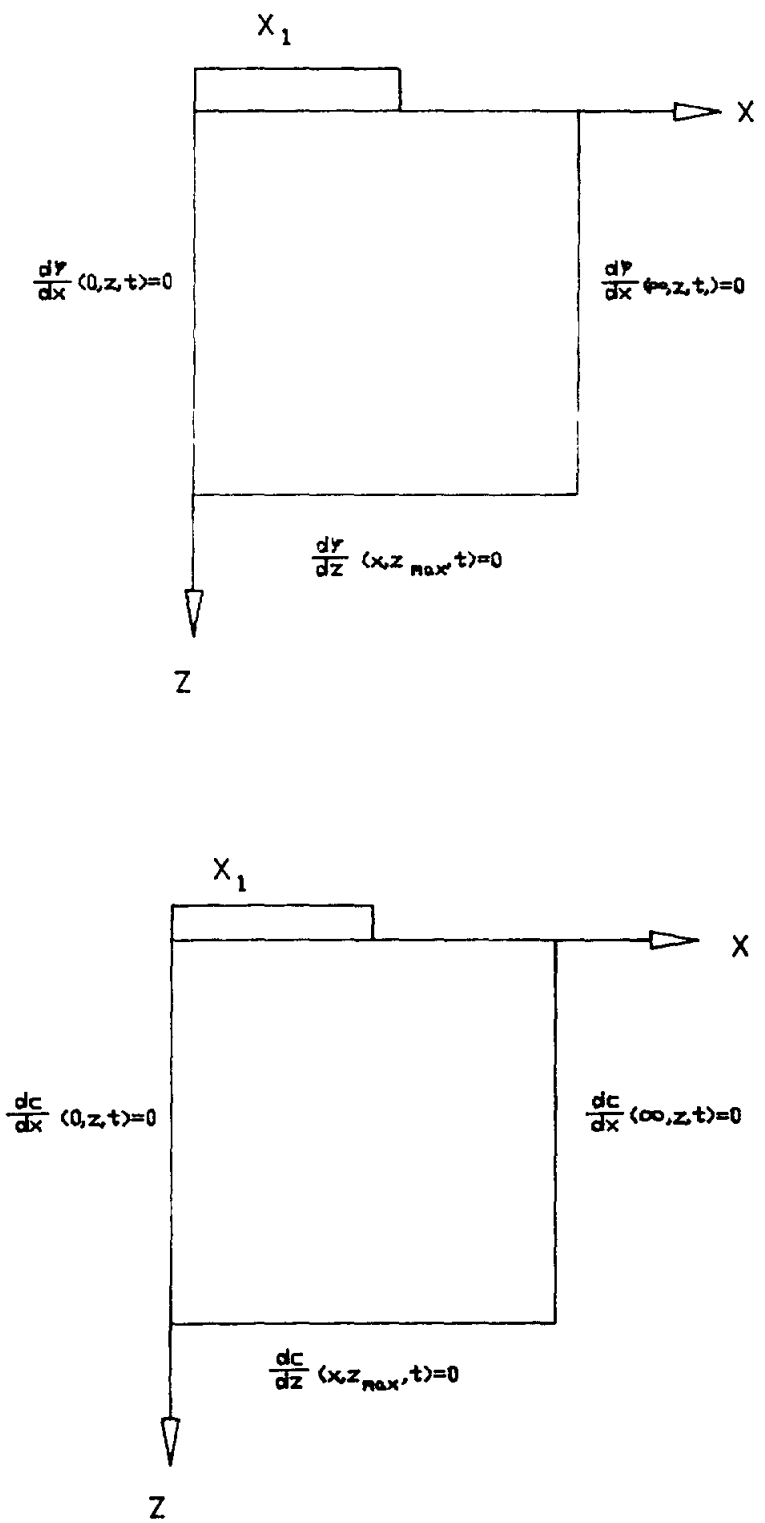


Figure 3. Initial and boundary conditions for the flow equation (TOP) and solute transport equation (BOTTOM).

$$D_x \frac{\partial^2 C}{\partial x^2} + D_z \frac{\partial^2 C}{\partial z^2} - V_x \frac{\partial C}{\partial x} - V_z \frac{\partial C}{\partial z} - \lambda RC = \frac{\partial C}{\partial t} \quad [7]$$

Where C = concentrations of solute (M/L³)
 D = dispersion coefficient (L²/T)
 V = velocity component (L/T)
 R = retardation factor, dimensionless
 t = time (T)
 λ = reaction constant (dimensionless).

Assuming a conservative solute and neglecting molecular diffusion, the basic transport equation reduces to Equation [8],

$$D_x \frac{\partial^2 C}{\partial x^2} + D_z \frac{\partial^2 C}{\partial z^2} - V_x \frac{\partial C}{\partial x} - V_z \frac{\partial C}{\partial z} = \frac{\partial C}{\partial t} \quad [8]$$

The dispersivity in Equation [8] is represented as follows (x-direction).

$$D_x = D_L \frac{V_x^2}{|V|^2} + D_T \frac{V_z^2}{|V|^2} \quad [9]$$

Where D_L = longitudinal dispersivity, (L²/T)
 D_T = transverse dispersivity, (L²/T), and
 $|V| = (V_x^2 + V_z^2)^{0.5}$

Numerical Solution Procedure

The flow equation was estimated by using a central difference scheme in the X and Z directions while applying the initial boundary conditions as shown in Figure 3 (Acharya, 1986). The initial and boundary conditions for the transport equation are also shown in Figure 3. An implicit procedure was utilized to solve for both the flow and solute transport equations simultaneously and the velocity was calculated by Darcy's Law. The main reason for using this method was the applicability of its use by microcomputers.

GROUNDWATER TRACER TEST

Field Layout Design

The test site layout, consisting of ten observation and one injection well in the Ogallala aquifer, was designed primarily from on information obtained from existing wells in the area and from limitations imposed by structures and

activity on the site. Figure 4 shows the location of the test well field in relation to pumping wells and landmark buildings in the area. It should be noted that three pumping wells already existed on the site, each pumping continuously as part of the campus water table control program. The "biology" well was identified as the well most probable to have an impact on the groundwater flow direction because the rate of pumping (approximately 190 gpm) was considerably higher than that at the two other wells.

From the information obtained from the three area pumping wells, other area observation wells and historical data from the Office of Water Management at Texas Tech University, the local natural gradient at the test site appeared to be in a northeasterly direction. The gradient direction was only slightly different from the direction of the injection well to the "biology" well. This led to the layout of the observation wells in a line from the injection point toward the "biology" well. Figure 5 shows the layout of the observation well grid with Well B as the tracer injection point. The small well spacing (25 ft) around the injection point ensured adequate tracking of the tracer peak during the early portion of the test. The number and pattern of the wells was chosen to optimize the project funding.

Well Construction and Installation

Each well was constructed with a 6 inch rotary bit attached to the end of pipe sections 5 feet in length similar to using the hydraulic rotary process (Driscoll, 1986). During the drilling process, soil samples were collected from several wells, and drilling rate was recorded to allow for at least minimal identification of the geological formation. Figure 6 shows the profile as interpreted from soil samples and area well logs. As expected in alluvial materials, marked interbedding of sand, sandy clay, and caliche was observed. The vertical variations that was noted could significantly affect tracer movement.

A continuous layer of caliche was encountered at each well, usually beginning at a depth of about 5 to 10 ft below the ground surface (Figure 6). The thickness of the caliche varies significantly in both the North-South (Wells A-L) and East-West (Wells C-E) directions. Along the section from Well A north to Well L, the caliche layer thickness varies from 7 to 14 feet. Below the caliche are apparently interbedded layers and lenses of sand, white sandstone, and sandy red clay. These variations can easily affect the movement of groundwater and the tracer in both the horizontal and vertical directions. The thickness of the caliche layer varied most dramatically along the section from Well C East to Well E (Figure 7). While the sand, sandy red clay, and sandstone seen at other wells were also found at Well C, it was impossible at Well E to locate the lower limit of the caliche layer within 60 feet of the subsurface. The caliche at Well E was very difficult to drill through, especially 20 to 25 feet below the surface. This tight caliche material appeared to be indurated and indirectly indicated that the aquifer was much less permeable along the eastern portion of the test site. The distribution of the interbedded layers between Wells D and E are only estimated as pinching out in Figure 7, since the layers were not encountered at Well E.

The saturated thickness of the Ogallala aquifer beneath the TTU campus is approximately 110 ft (Chen, 1987). Project funds did not allow the installation of wells to a depth sufficient to reach the confining clay "red

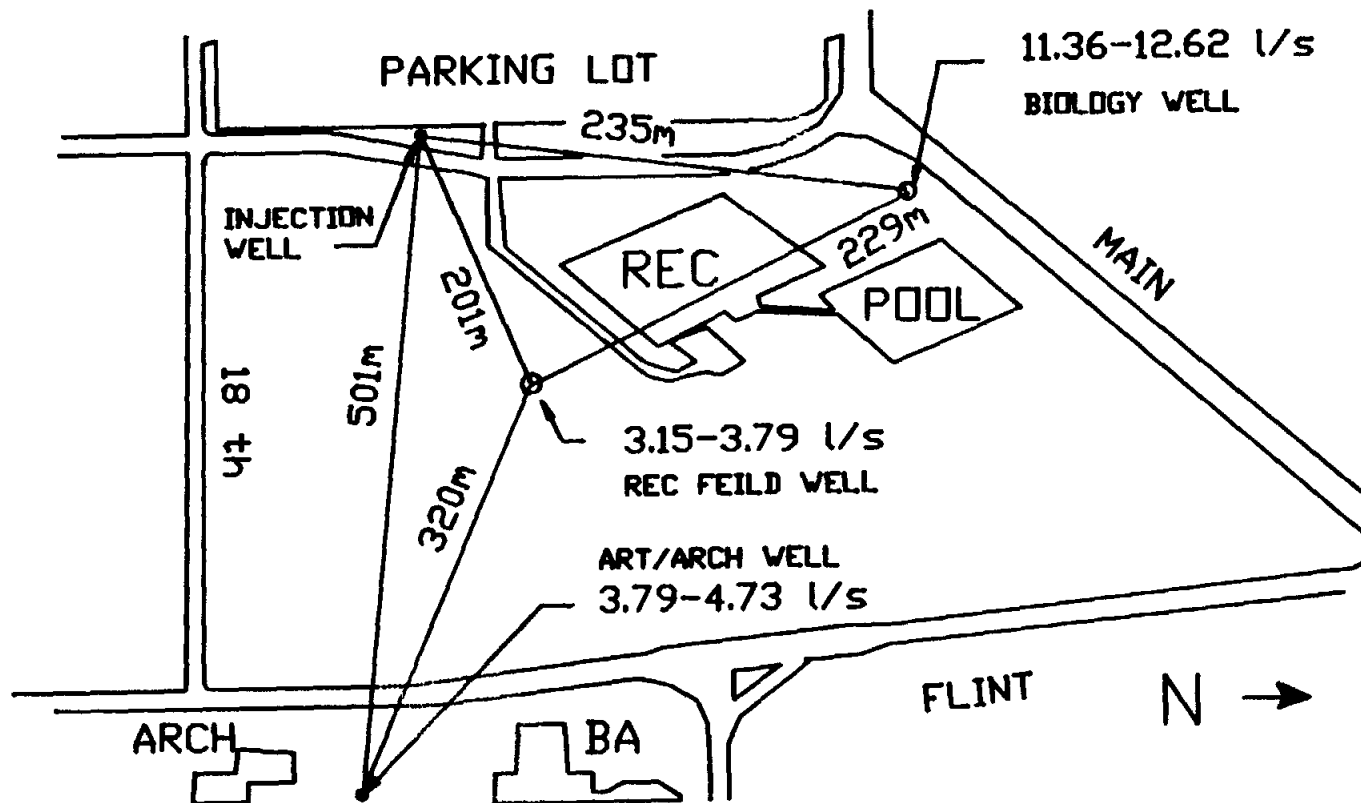


Figure 4. Location of well field in relation to area landmarks.

N →

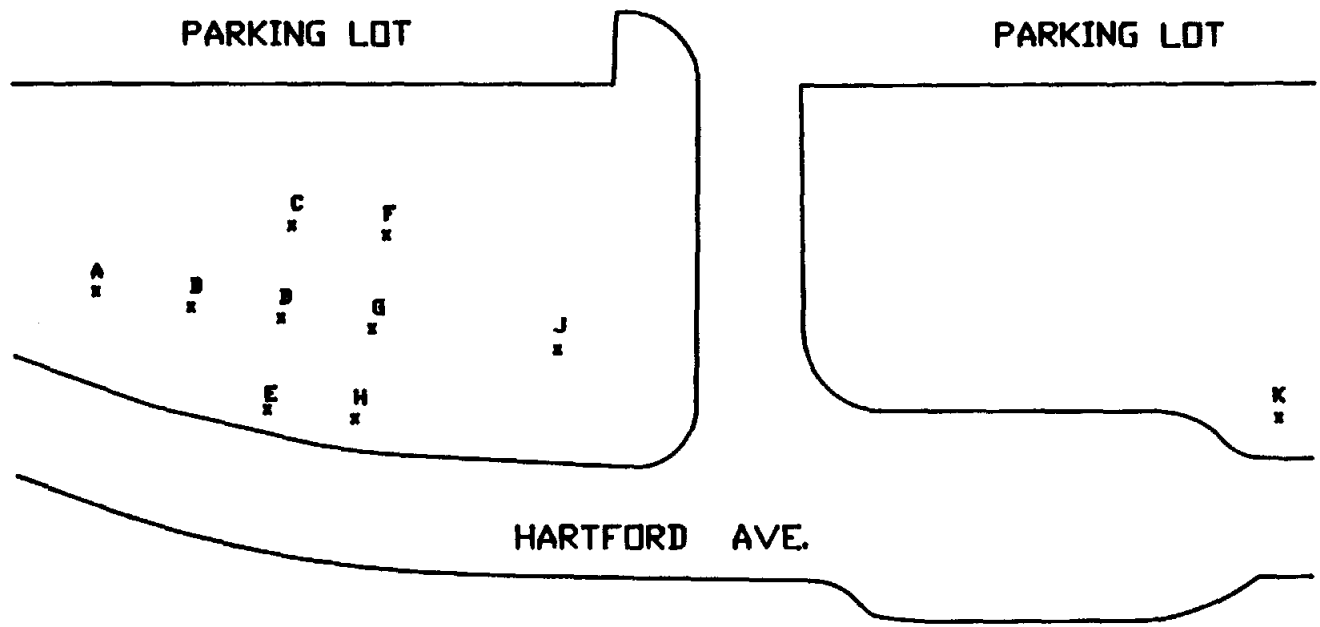


Figure 5. Layout of the wells used in field study.

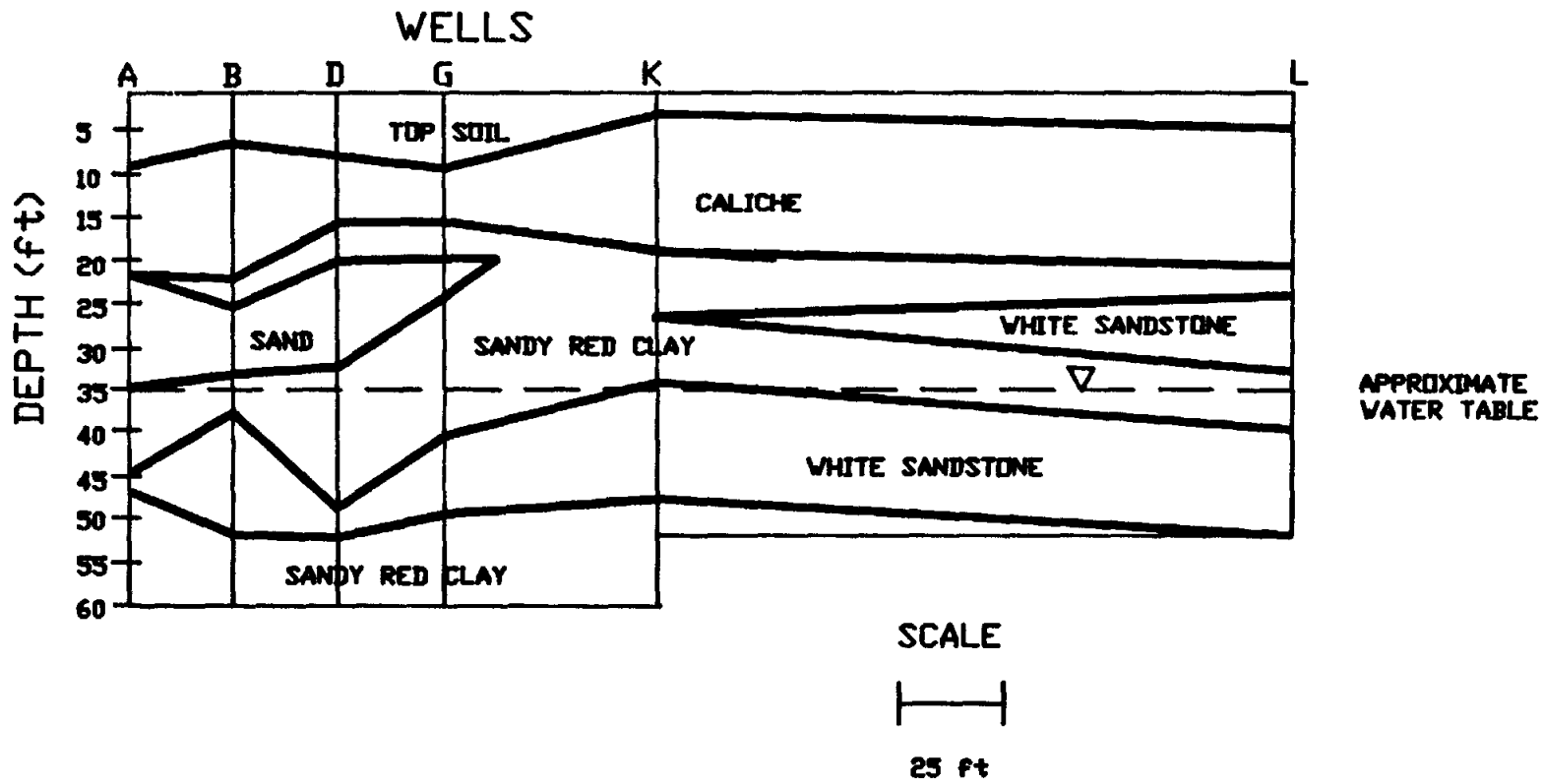


Figure 6. Estimated geological formation profile for line from Well A to Well L.

beds" beneath the Ogallala. Since the vertical movement of solutes in groundwater is usually small relative to the horizontal advection and dispersion (Freeze and Cherry, 1979), a decision was made to drill the wells for this project only into the upper third of the saturated thickness. It was recognized that significant vertical migration of the tracer could greatly affect the interpretation of the monitoring data.

The observation wells were drilled to a depth of approximately 63 to 65 ft. from the ground surface. All wells were cased with 2 in. I.D. PVC pipe to a depth of 60 ft., which allowed room at the bottom of the bore hole for sediment deposition. The well casing was perforated with rectangular slits beginning at a depth of 30 ft. and extending to the bottom of the casing.

The injection well (B) was constructed in a similar manner using an 8 in. drill bit. The well casing was perforated from 30 to 50 ft. with a solid cap at the bottom of the pipe to prevent vertical flow during injection. An envelope of small uniform gravel was placed around the injection well casing to enhance uniform tracer distribution.

Following installation, each well was flushed using a high volume of municipal water to remove solid particles from inside the casing. After flushing, the wells were either bailed or pumped to remove any effects of dilution caused by the water added during the flushing process. Several weeks were allowed to pass between the installation period and the start of tracer injection to insure the aquifer was at normal conditions and sufficient baseline water quality data could be collected. The natural bromide concentrations in the 10 test wells ranged from 1 to 4 mg/L, with an average of 2 mg/L.

A total of 11 wells were originally planned, but well L could not be completed because of limitations in the drilling rig that was available for use in the project. In all, nine observation wells were used to observe the movement of the tracer from the injection well. Although the flow direction was assumed to be in the line from well B to K (Figure 6), wells A, C, E, and F were included to detect any deviations of tracer movement away from the assumed flow direction. The normal water table was relatively level in this area, so transverse movement was possible.

Tracer Injection

There are many non-reactive tracers that have been used by researchers, with Cl and Br as the most common (Davis et al., 1980). Due to the high level of Cl present in the aquifer, bromide was selected as the tracer for this study, with sodium bromide (NaBr) used as the Br source.

It was estimated, with the use of the computer simulation program described in a later section, that a 24-hour injection period at a Br concentration greater than 1 g/L would provide sufficient Br for detection at each of the observation wells, assuming uniform aquifer conditions. In order to accomplish a continuous 24-hr injection period, two storage tanks were used to hold the NaBr mixture. Each tank was connected to the injection pump by PVC pipe and a valving system (Figure 8). During the injection period, one tank was being prepared with the tracer solution while the solution in the other tank was being injected into the aquifer. To ensure that the NaBr remained in

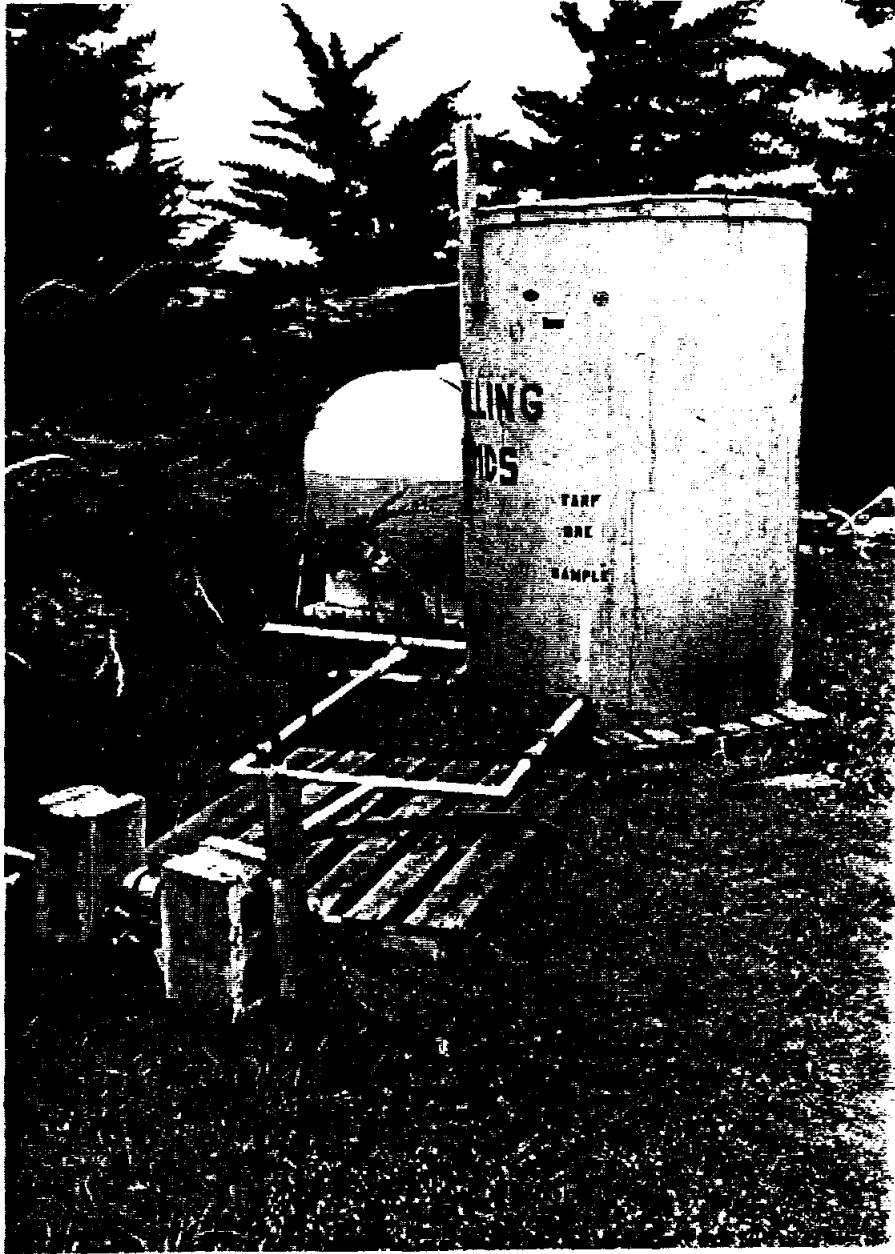


Figure 8. Equipment used during tracer injection.

solution, a re-circulation pipe was connected to the output side of the pump and the pumped tank. The valving system was arranged so that the injection remained continuous at a rate of 2 gpm. During the injection period, six tracer solution batches were required with the average injected Br concentration being 4350 ± 340 mg/L.

Groundwater Sampling

At the midpoint and end of the injection period, the water table elevation was monitored and water samples were collected from each observation well to examine the effects of injection on the aquifer. After injection, water samples were collected twice daily from each observation well during the first week. This high sampling frequency was used to ensure that the peak Br concentration plume could be identified as it passed the observation wells closest to the injection point. As the changes in Br concentration became smaller, the sampling frequency was reduced to daily, three times a week, twice a week, weekly, and biweekly. The total sampling period was approximately 300 days. Water elevation measurements were made occasionally to note changes in aquifer water level during the test period.

Water samples were collected from each well with a PVC bailer. Approximately two or three well volumes of water were removed from the well prior to sampling in order to obtain a representative sample of water from the aquifer. The plastic sample bottle was then rinsed with the bailed water before each sample was collected then the bailer was lowered to approximately 55 ft below the ground surface to collect the sample. All samples were stored at 4 degrees C until analysis, usually within less than week after collection (APHA, 1985).

Sample Analysis

Well water samples were analyzed for Br concentration with the use of a Dionex 2010i ion chromatograph (IC). The column used was an IONPAC HPIC-AS3 (Dionex Corp). Each water sample was filtered using a vacuum filter system equipped with a GN-6 metrical membrane filter with a pore size of 0.45 microns. Samples were diluted with distilled water when necessary, so that sample Br concentrations were within the detection range. At least two aliquots of each filtrate were injected into the IC for Br determination to ensure statistically representative samples.

Modeling Field Tracer Movement

Several computer programs have been developed in the past fifteen years for modeling solute transport in porous media. These models have been useful in translation of solute movement data into detailed description of hydrogeologic environments, and in the prediction of potential migration of contaminants. One program, referred to as the USGS-2D model, developed by Konikow and Bredehoeft (1978), has been used by environmental engineers and hydrogeologists around the country. Since the USGS-2D model has come into general use with some success, it was chosen for this project. This next section of the project report includes a brief discussion of the capabilities of the USGS-2D model.

The USGS-2D Model

Konikow and Bredehoeft (1978) originally assembled this program to simulate the movement of a conservative solute through a two-dimensional flow field. The solute can move by both advection due to the bulk groundwater flow and by dispersion due to mixing caused by the tortuous flow paths within the porous medium. The aquifer of interest is discretized as a rectangular grid system, with each node in the grid representing local hydraulic and concentration values. First, for each time step, the program solves Equation [10] for two-dimensional flow through a heterogeneous anisotropic aquifer.

$$\frac{\partial}{\partial X_i} T_{ij} \frac{\partial h}{\partial X_j} = S \frac{\partial h}{\partial t} + W \quad i, j = 1, 2 \quad [10]$$

where T_{ij} = the transmissivity tensor (L^2/T)

h = hydraulic head (L)

S = storage coefficient (dimensionless)

t = time (T)

X_i, X_j = space coordinates, and

W = volume flux per unit area (+ inflow, - outflow) due to pumping or recharge (L/T).

This equation is discretized into finite-difference form and solved by an iterative alternating direction implicit procedure. The resulting head distribution is then used to calculate local velocities. Next, the program solves the two-dimensional Equation [11] for dispersive transport of a nonreactive solute.

$$\frac{\partial (Cb)}{\partial t} = \frac{\partial}{\partial X_i} (b D_{ij} \frac{\partial C}{\partial X_j}) - \frac{\partial}{\partial X_i} (b C V_i) - \frac{C'W}{\epsilon} ; i, j = 1, 2 \quad [11]$$

where C = solute concentration (M/L^3)

D_{ij} = hydrodynamic dispersion tensor (L^2/T)

b = saturated thickness of the aquifer (L)

V_i = velocity in X_i direction (L/T)

ϵ = porosity (L^3/L^3), and

C' = solute concentration in a fluid source or sink (M/L^3).

The dispersion tensor is defined by the directional components of the longitudinal and transverse dispersivities, D_L and D_T , and the local velocity magnitudes. The transport equation is solved using the method of characteristics, simulating solute movement by tracking the movement of hypothetical particles through the flow field. Details of the solution techniques are provided by Konikow and Bredehoeft (1978).

The major assumptions of the model must be recognized as possible limitations of its applicability and are summarized as:

1. Darcy's law is valid, and hydraulic head gradients are the only mechanism for fluid flow.
2. Porosity, storage coefficient, and hydraulic conductivity are constant in time, and the porosity and storage coefficient are uniform in space.
3. No chemical reactions affect the solute concentration, fluid properties, or porous medium.
4. Molecular diffusion is negligible.
5. Head and concentration do not vary in the vertical direction.
6. The longitudinal and transverse dispersivities and the hydraulic conductivity anisotropy factor are constant throughout the aquifer.

Once the aquifer area is fitted with a rectangular grid, the program accepts values of transmissivity, saturated thickness, water table elevation, diffuse recharge, and background solute concentration at each node. The program treats the aquifer as uniform in longitudinal dispersivity, ratio of longitudinal and transverse dispersivity, ratio of the local transmissivities in the two principal directions, porosity, and storage coefficient, and accepts single values for each of these parameters. Pumping or injection wells may be located at any node, and observation wells may also be chosen. Transient or steady state flow conditions may be simulated. Constant head or no-flow boundary conditions may be specified.

Other users of the USGS-2D model have noted that the model results are quite sensitive to a few of the parameters. Davis (1986) and Chapelle (1986) recognized the interaction between areal transmissivity variations and dispersivity. Both researchers were concerned with alluvial aquifers which were very heterogeneous with respect to transmissivity due to interbedding of gravels, sands, and clays. If the transmissivity variations within such an aquifer are not accurately discretized, large dispersivity values on the order of hundreds of feet may be needed to best simulate measured data and may not provide satisfactory approximation of the observed concentration changes due to excess spreading of the model solute plume. When the transmissivity is accurately represented by a fine grid, much better agreement between observed data and calibrated model simulations is possible, with much smaller values of dispersivity. This is not unreasonable since the dispersion coefficient is a product of both velocity and dispersivity. Uncertainty in one of these two values affects the value of the other required for accurate modeling. It is impossible to remove all uncertainty from either value due to the difficulty in obtaining sufficient physical data about every point within a subsurface investigation. The Ogallala aquifer, in which the tracer test in this project took place, is also an alluvial formation. As reported in an earlier section of this report, wide variations in aquifer material were encountered within an area of less than one half acre.

RESULTS AND DISCUSSION

EROSION CHARACTERISTICS

Wind Erosion Model

The wind erosion model developed by Gregory and Borrelli (1986) was used to simulate the transport of a potential chemical by wind. Results of the model showed that a chemical concentration ratio (CCR) ranged from about 1 to 4 for the soil particles up to 1 mm in size, as used in the tests. The CCR is defined as the area divided by the mass of the material moved divided by the ratio of the area and mass of the available material in the test cell. This is similar to the results found by researchers at the USDA-ARS laboratory in Big Spring, Texas (Donald Fryrear, personal communications, 1988). At the wind velocity of 8 m/s (17.9 MPH) the CCR simulated for soil without a clod cover was 2.1 with a U_{*c} value of 0.35 m/s. For the situation with clods, the CCR was 4.0 with a U_{*c} value of 0.35 m/s. Dividing the CCR value with clods by the CCR without clods gives a value of 1.9, which means that the overall concentration of the chemical found in wind erosion samples where clods are present would be 1.9 times greater than that found from the test where no clods were present. This increase in the CCR shows the deposition of the heavier (larger) particles and the transport of the smaller more numerous particles. When summing the total cross-sectional area (where the potential chemical is attached) of transported particles, the smaller particles will transport more total chemical per mass of soil moved. This interaction helps explain the fact often observed that a small amount of clod cover in the field can be more damaging than no clod cover. Of course, as the surface becomes inundated with clods or other type of cover, soil movement will cease.

Further interaction of the pollutant with water follows by washing or dissolving the chemical, continuing movement, whether across the surface to a stream or to the groundwater via infiltration or some direct pathway. These types of interactions are highly variable and very difficult, if at all possible, to actually measure. Generally, a combined effect of several factors are measured and a conclusion is inferred based on those results. Unfortunately, these inferences cannot be extrapolated to other sites with a high degree of confidence and, therefore, should be viewed with caution.

Wind tunnel tests performed with soil similar to that used in the model simulation described above resulted in an average change in phosphate concentration ratio (chemical concentration ratio) of 1.1 (an actual concentration of 1630 mg P/kg soil) when no clods were present. Theoretically, the ratio should be 1.0 if there were truly no clods. The fact that some dissolution or aggregation of the soil could have occurred would account for the ratio to be slightly greater than unity. When clods were present at a 30 percent fraction of surface cover, the phosphate concentration increased from 1205 to 2320 mg P/kg soil, or an increase of 1.93 times the initial concentration. This result is in agreement with the simulation model thereby providing a valuable method of estimating the fraction of chemical movement due to wind.

Results from the wind tunnel studies indicate that the wind erosion model can be used to predict chemical movement (Gregory et al., 1988) with soil via erosion by wind. Since often times the eroded soil will deposit in low lying

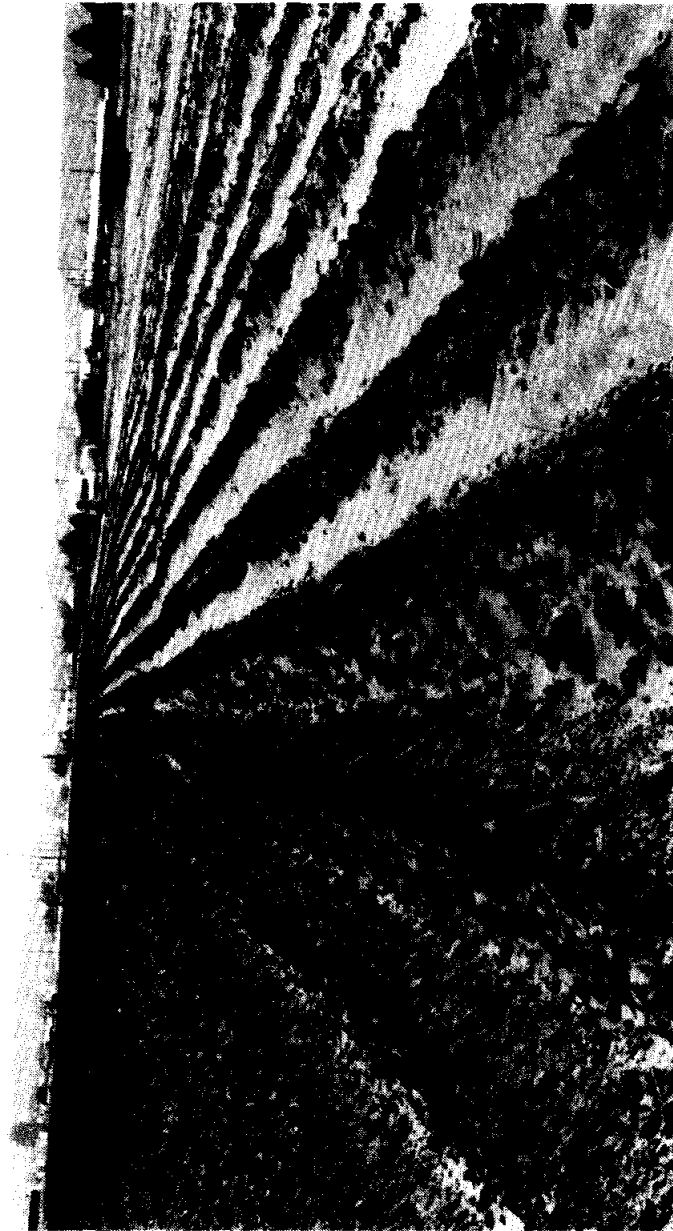


Figure 9. The effects of wind erosion on a bare field with ridges.

areas (Figure 9), the potential for creating chemical "hot spots", or increased chemical concentration than that applied, does exist. For chemicals such as Trifluralin, Paraqual, Propazine and others that persist in the soil for more than 100 days (Ristau, 1982) and those that are highly soluble, the potential for further movement from the low lying areas, possible to groundwater, can be high.

Field Deposits

The field study was initiated by examining the 5-year history of chemicals used at the various locations. The resulting chemicals (pesticides) used were Treflan (primary herbicide), Caparol (prometryme), Propazine (only minimally), Fusalane (banded), and Temik (banded). Tests from the soil samples collected revealed only Treflan to be available in measureable quantities (which is reasonable since it was the most widely-used chemical on all plots), therefore efforts were concentrated on detection and potential movement of Treflan. Another reason for no detection of the insecticides, for example, was due to the highly reactive, both biologically and photosynthetically, chemicals that were used on the plots.

To determine a baseline for Treflan (Trifluralin) concentration at the field study test areas, a test plot where no crop has been grown nor chemical application had been made for at least 2 years was examined. Tests showed that some residual chemical was present in the soil at a level of 0.16 mg Trifluralin per kg of dry soil. The concentration found after incorporating the Trifluralin with an application of 1 qt/ac was 3.4 mg per kg of dry soil. With these two boundary conditions for chemical concentration, the three deposit areas, as shown in Figure 2, were examined.

Erosion sample areas A, B, and C were sampled on the first day following an erosion event where both high winds and rain existed. In this case, the first erosion event occurred approximately 5 weeks after planting and chemical application. In the two areas A and B, the concentration of Trifluralin found was only slightly higher than the base concentration at 0.2 mg Trifluralin/kg of dry soil. This was not significantly greater than the base concentration ($\alpha < 0.05$), but it indicates the potential for movement does exist. These results are similar to more controlled experiments where a time span of over 4 weeks were allowed between chemical application and sampling (Triplett et al., 1978; Leonard et al., 1979; and Haith, 1980). Significant levels of chemical were found by the investigator in the erosion sediment only if the erosion event (usually by water) occurred within one week after chemical application. Yet, in all cases, small amounts of chemical were transported after several weeks had passed. Again, the potential for chemical movement by erosion does exist and can be a major factor in identifying whether or not non-point source pollution from agricultural chemicals is occurring.

Sample site C showed no movement of Treflan from the field during the test period. This result was expected because the land was terraced for control of erosion by water and a residue remained on the soil surface (restricted tillage) to help prevent erosion by wind. In this case, only a very small amount of erosion was detected and that soil had an average Trifluralin concentration of 0.14 mg/kg of dry soil, which was not statistically different ($\alpha < 0.05$) from the base concentration. This test site shows that if proper erosion control measures are practiced by a producer,

little to no transport of surface applied chemicals would exist, thus reducing the possibility of surface or groundwater pollution from the applied pesticide.

2-D UNSATURATED FLOW MODEL

Vertical Solute Movement Simulation

The main purpose of this portion of the study was to develop a computer program (Appendix A), suitable for typical microcomputers that could be used to estimate the two-dimensional movement over time of a conservative solute applied to the soil surface. The soil system, or grid, was uniformly divided into a number of nodes in the X and Z directions. Water and solute were applied to the soil surface over a specified distance in the X-direction of the chosen grid. It was assumed that the surface layer was saturated for a specific time. For the purpose of this study, the initial solute concentration was chosen to be 100 mg/L and the longitudinal dispersivity was 0.1 ft²/d, typical for soils in the Texas High Plains. The ratio of the transverse to longitudinal dispersivity was assumed to be 0.3.

Three soil types were examined for solute movement with the use of this program. Efforts were concentrated on the Amarillo Silt Clay soil because it is a significant Texas High Plains soil type. The other two soil types were Poudar River Sand and Fine Sand. The soil characteristic data for these soils (as shown in Appendix B) were provided by the Water Resources Center at Texas Tech and is reported by Maulem (1976).

Since the Texas High Plains contains numerous playa lakes with soil types similar to the Amarillo Silt Clay, the simulation test was devised to examine the fate of a pollutant that was transported to the lake by erosion. In this case, it was assumed that water remained in the lake for 60 days and the solute concentration was 100 mg/L. The solute concentration is higher than that most likely found, but it allows tracking of the solute and is a direct multiple of an actual application. To simulate the worst-case scenario, the solute/soil interaction was assumed negligible. For the case of water soluble chemicals, this assumption would be valid, yet other chemicals (e.g. atrazine) will bond to soil particles and resist movement until sufficient water movement can strip it from the soil.

Figure 10 shows the solute concentration contours for the 30th, 45th and 60th day of the simulation period. Note that the simulated area is in the x (horizontal) and z (vertical downward) directions with the grid beginning in the upper left corner of the plot. The total contour to the left would be a mirror image of that found to the right of the x = 0 line on the plots (the left side). Under uniform application and flow, the solute moves approximately 4 ft. vertically and 3 ft. in any direction horizontally at a concentration 20 times less than the initial concentration. It would appear that the unsaturated soil has a high capacity for containing the water and solute causing movement to be slowed and quite confined. For most pesticides used by the farmers, the slow movement should provide adequate time for the chemical to degrade or be reduced to a non-polluting level.

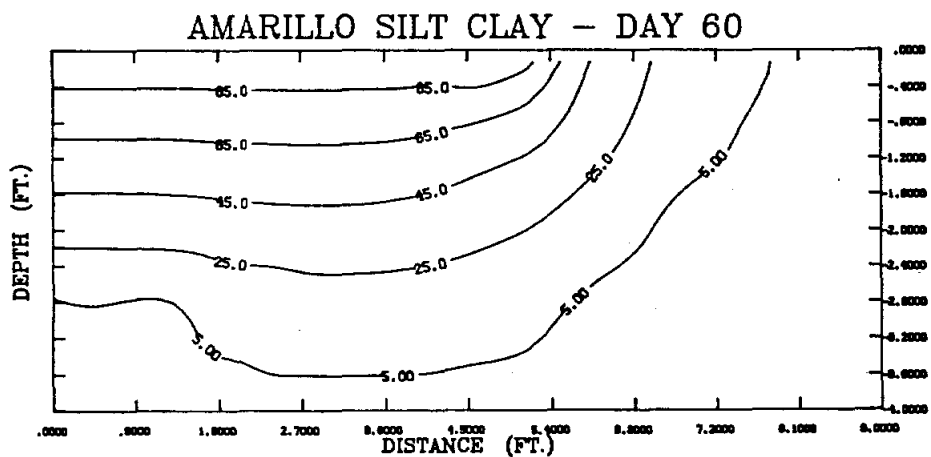
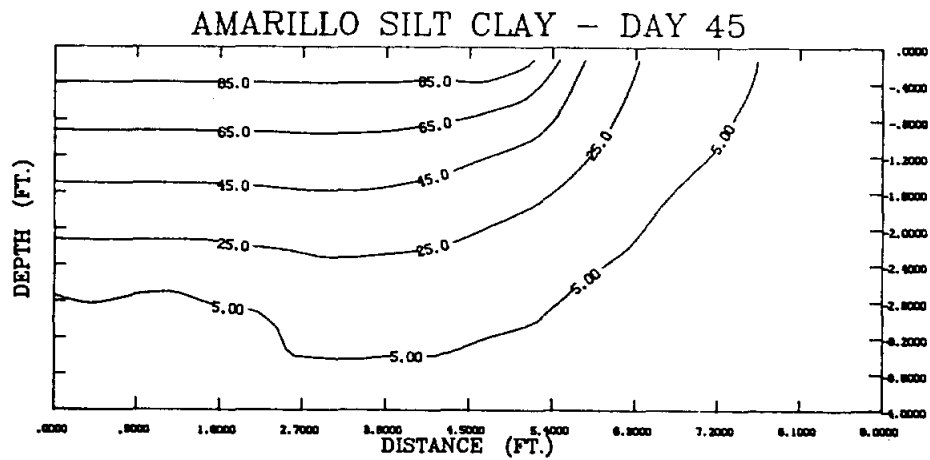
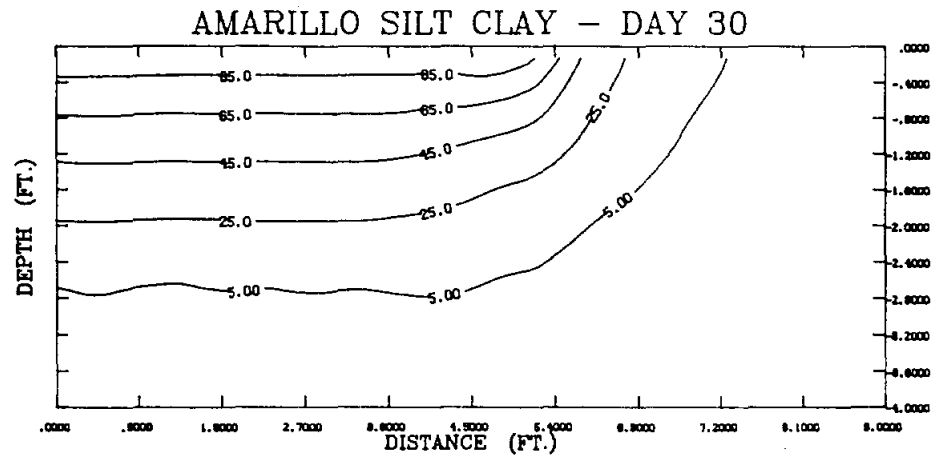


Figure 10. Simulated concentration contours from the continuous tracer application to unsaturated soil.

The simulation of the playa lake case also points out other facts. Even though the solute was reduced greatly and moved only a short distance in the simulated case, repeated action of the loading process for persistent chemicals could move that chemical toward groundwater in a short time. This repeated loading type of condition should be examined further. Also, it is obvious that chemicals applied to the ground surface, for example by the farmer, will not directly be transported to groundwater. Transport mechanisms, such as erosion, must concentrate the chemical first in an area which promotes vertical movement. Another alternative pathway for the chemical to reach groundwater is more direct, either through well holes or possibly a macropore soil system that doesn't follow Darcy's Law for movement.

GROUNDWATER TRACER TEST

Tracer Test Results

After installation of the injection and monitor wells, the test site was left undisturbed for more than a month to allow the water table and water quality to return to baseline conditions. On August 19, 1986, an injection attempt was begun at an injection rate of 10 gpm, based on typical estimates of transmissivity for the local Ogallala. This attempt was aborted after less than 20 minutes when it was found that the injection well could not accept this flow rate. Less than 200 gal of Br solution were injected during this brief period, which caused some small but noticeable changes in the Br concentrations in wells A, B, C, and D. These data are shown in Table C1 in the Appendix. It was decided to inject at a flow rate of 2 gpm since a computer simulation with estimated hydraulic parameters showed that measurable concentration changes at the monitor wells could be caused by introducing a concentrated Br solution at the 2 gpm flow rate for 24 hours. Practice injection of tap water at 2 gpm during the well development period also demonstrated that that flow rate could be accepted by Well B for a reasonable duration.

The actual tracer experiment began on August 29, 1986, and the tracer solution was successfully injected at Well B for 24 hours at a constant rate of 2 gpm. A total of six tanks of solution were mixed during that day, at an average measured Br concentration of 4350 mg/L. Table C1 in the Appendix provides the Br concentrations measured at Wells A-K, from 18 days prior to the 24-hour injection to 297 days afterward. Blanks in the table indicate that the data were not available due to sampling or analytical problems. In Figure 11, plots of the concentration histories at the wells are arranged in a manner similar to the orientation of the wells at the site. This allows visual comparison of the changes in Br concentration in all the wells over time. Since Well B, the injection well, was the only well to have concentrations approaching the injection concentration of 4350 mg/L, a common concentration range of 0 to 200 mg/L was used to allow simple qualitative comparison of the changes at the various wells. Even though there is some scatter in the data, it is possible to discuss overall trends.

Inspection of Figure 11 demonstrates that the Br plume did not move directly along the line from Well B to K, but part of it appeared to veer eastward around Well D towards Wells E and H, where it remained for much of the test period, while another portion traveled quickly to Well G. The peak concentration at Well D was only 50 mg/L, 35 days after injection. After

rising quickly, the Br concentration at Well D fell back below 10 mg/L within 90 days. At Wells E and H, the Br levels rose above 90 mg/L after 50 days. The concentration at Well E rose slowly to 120 mg/L about 110 days after injection, then decreased below 20 mg/L by 250 days after injection. At Well H, the concentrations seemed to oscillate between a maximum of 120 mg/L and a relative minimum of 40 mg/L for the duration of the monitoring period. The greatest Br concentration, over 170 mg/L, was measured at Well G approximately 50 days after injection. After 100 days, the Br level at Well G dropped below 10 mg/L.

The Br concentrations at Wells A, C, F, J, and K all showed much less variation than the wells previously discussed. Well A, up-gradient from the injection well, varied somewhat erratically from 2 to 8 mg/L over the test duration. The Br concentrations at Wells C and F rose to about 14 mg/L at 30 and 50 days, respectively, after injection before declining back to baseline values 150 days after injection. Well J showed a peak concentration of approximately 10 mg/L after a slow rise 120 days after injection before returning to baseline values. The concentration at Well K peaked at approximately 14 mg/L at 130 days after injection, then dropped quickly back to 2 mg/L.

The Br concentrations at the injection point, Well B, were measured at above 3500 mg/L for the first few days after injection, before falling below 100 mg/L about 40 days after injection. Even at Well B, the Br levels returned to the baseline value of approximately 2 mg/L about 170 days after injection.

The movement of the Br tracer through the test site was different than that previously estimated from examination of the local water table elevations in the test site area. One possible explanation is the effects of stark differences in permeability within the test site, as is often encountered in alluvial aquifers. While expected to move northward from Well B directly toward Well K, the tracer plume took a definite northeasterly path. In addition, the tracer peak did not even pass through Well D, the well closest to the injection point, but did come around Well D and pass through Well G. This could indicate a zone of low permeability around Well D which deflected the plume to the east, accompanied by a channel of high permeability which connected Well B and Well G. The relatively long residence time of elevated Br concentration at Wells E and H could be caused by the existence of another low permeability zone which arrested the plume once it reached those wells. The small concentration changes seen at the other wells demonstrated that the peak of the plume did not pass near those locations. The vertical orientation of the sandy clay, sand, sandstone, and caliche layers could also affect tracer migration as water seeks the path of least resistance. The permeability differences were explored in the modeling effort, described in the following section.

Another possible explanation of the changing direction of plume movement could be local variations in the elevation of the water table which could reverse the local head gradients. As presented in Table 1, the depth to water in the test wells moved up and down approximately one foot during the study period. In Table 1, the depths to water for Wells A-K are shown for a few representative dates during the test period. The data demonstrate that the water generally fell or rose in all the wells between measurements. For example, between 8/30/86 and 2/30/87, the depths to water increased at 8 of the

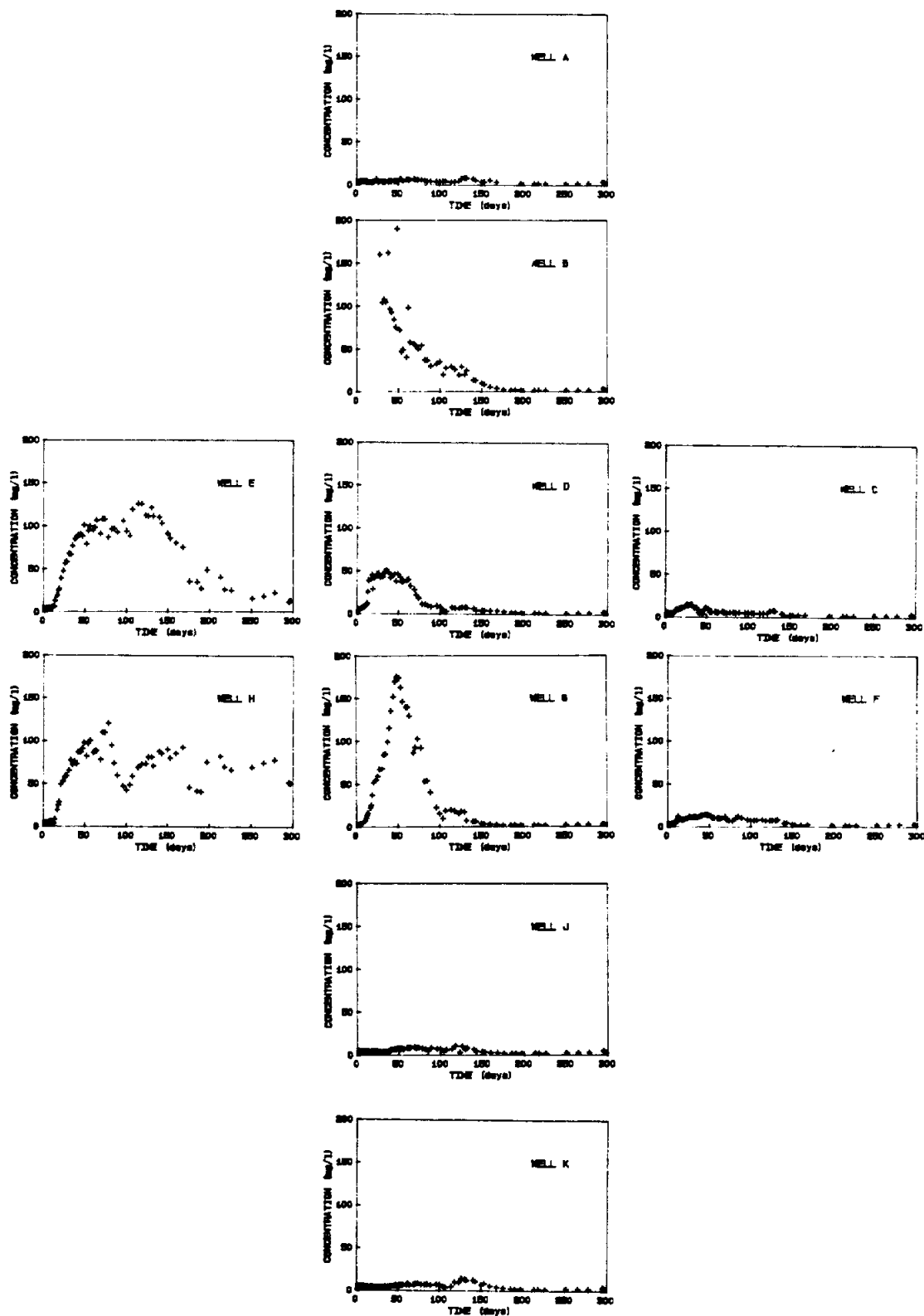


Figure 11. Bromide concentration histories for Wells A through K arranged as in the field.

10 wells, with Well D showing no change. Between 2/20/87 and 5/31/87, the depths to water in all 10 wells increased. The average depth to water for the study period is shown in the final column. Since the water table was only 30-35 ft below the ground surface, nonuniform infiltration from the surface could possibly affect the water table. However, this is unlikely, since the test site exists in a small area bounded by a two-lane paved street with storm gutters and a paved, well-drained parking lot. Virtually all storm runoff was removed from the site by surface drainage, with little water left for infiltration. In fact, the depth to the water table generally increased in all the wells during the 300-day study period. Attention to this phenomenon is discussed in the following section, which describes the modeling techniques.

Table 1. Measured depths to water table from the surface in test wells during study period.

Well	Depth to Water			Average Depth, ft.
	8/30/87	2/20/87	5/31/87	
A	34.4	34.5	34.8	34.6
B	34.8	34.6	35.3	34.9
C	34.5	34.7	34.8	34.7
D	34.6	34.6	35.1	34.8
E	34.4	34.7	35.1	34.8
F	34.5	34.8	35.1	34.8
G	34.6	34.7	35.0	34.8
H	34.6	34.8	35.1	34.9
J	34.7	35.0	35.4	35.1
K	35.4	36.2	36.7	36.2

The major conclusion that may be made from the tracer test results is that the movement of solutes in groundwater in this section of the Ogallala is difficult to predict. Estimation of the local head gradient from local depth to water measurements was not sufficient for accurate forecasting even in this small test site. Subsurface descriptions from the examination of drilled materials was somewhat helpful in identifying possible zones of different permeability, but these data are limited by the small number of discrete point locations within the site. When the solute is within a relatively permeable zone, it may travel at velocities on the order of feet per day. Pollutants could be very mobile in this situation, and unfortunately the more permeable zones cannot be located easily from the surface. On the other hand, when the solute reaches a zone of stiff material, it may remain there at relatively high concentrations for a significant period of time. Removal of groundwater pollutants from such a zone would be more difficult than from a zone in which the solute is more mobile. Both of these situations are important considerations for protection and restoration of local groundwater quality. Since the Ogallala is an important water resource for the High Plains of Texas, any pollutants which may enter the aquifer from human sources could be very difficult to track and to remove.

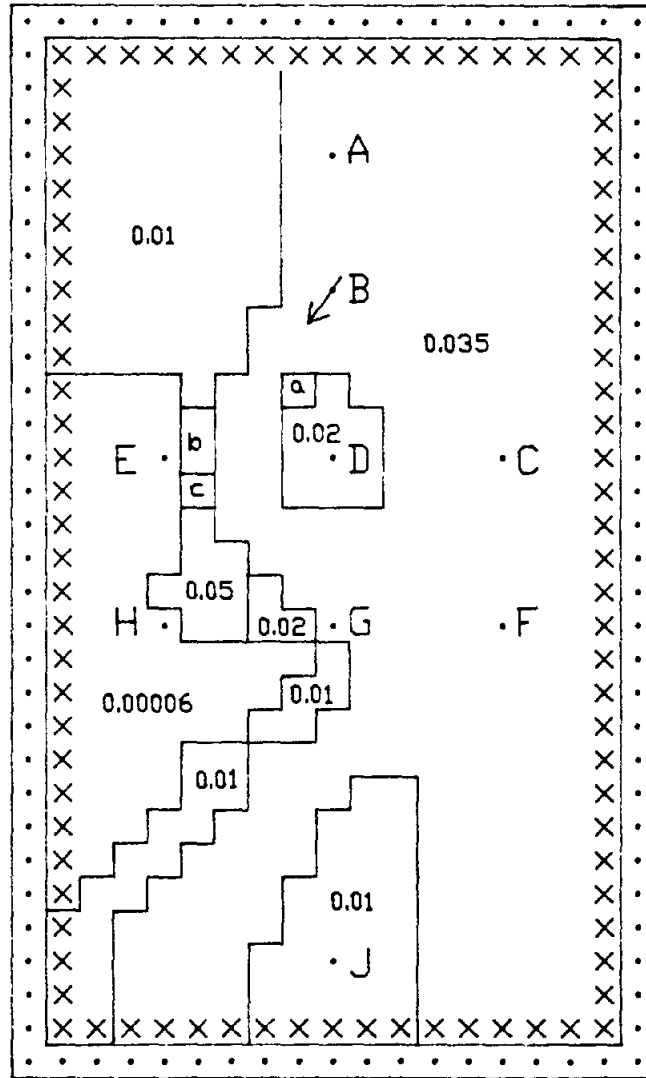
Model Setup

The configuration of the well field pattern and description of the site has been presented in a previous section of this report. Originally, the location was based on land availability and the hope that the general hydraulic gradient in the area would be defined by the pumping at the Biology well, which would encourage northward flow along a line connecting wells B, D, G, J, and K. The actual flow condition found at the site during the project, and verified by other well measurements near the site, was a more northeasterly gradient, which was due to a larger scale water table slope. Neither the Biology well nor the smaller well in the Recreation Center field appeared to affect the head distribution found by water depth measurements within the well pattern. The effects of the ore wells was also verified to be negligible by using the USGS-2D model and typical hydraulic parameters for the Ogallala to simulate flow in an area large enough to include the tracer site, the Biology well, and the Recreation Center well. It was virtually impossible to specify a combination of transmissivity and storage coefficient to allow the two pumping wells to cause measurable drawdowns in Wells A through J. For this reason, and since the bromide plume had moved quickly out of the well pattern toward the northeast, the aquifer areas simulated only included Wells A through J, and the hydraulic gradient was fixed by arranging constant head boundary nodes.

Figure 12 shows a general layout of the grid system used in the modeling effort. The transmissivity zones will be discussed with the modeling results. The total grid consisted of 19 nodes in the x-direction and 32 nodes in the y-direction. The distance between the nodes in both the x- and y-directions was 5 ft. The overall size of the grid was set to make sure that each well was at least three nodes from a boundary. The porosity for the entire area was set at a regionally typical value of 0.3. Typical storage coefficient, or specific yield, values for the Ogallala range from 0.15 to 0.25, so 0.20 was used in this study. The aquifer thickness was set at 30 ft, which approximated the length of well screen below the water table at each well.

As required by the program, the entire grid was surrounded by no-flow nodes. Just inside this mathematical requirement, constant head nodes were specified. The constant head values were set to insure a head gradient of 0.003 ft/ft in the x-direction and 0.006 ft/ft in the y-direction. The approximate elevation of the water table in the area had been located as part of another Texas Tech research project (Chen, 1987), at approximately 3195 ft above mean sea level. Using this as a base, the water table was specified at 95.6 ft on the southwest corner and 94.4 ft on the northeast corner of the grid, with intermediate values as required by the head gradient. Since the model was set up to allow only four digits to specify the head at each node, the values were input as actual elevation minus 3100 ft. With no pumping or recharge nodes, except during the bromide injection, the constant head boundaries kept the water table elevations at the monitoring wells very near the average values observed during the experiment, even with varying transmissivity values within the area. The actual and simulated water table elevations are compared in the discussion of the model results. The exact initial head values are shown in Appendix D as part of the sample input file.

The initial concentration of bromide in the aquifer was set at 2.0 mg/L throughout the site. This approximates both the background concentrations measured prior to the test and the final concentrations observed after the



a - 0.005 Transmissivities in ft /sec S = 0.20
 b - 0.02 x - constant head node n = 0.35
 c - 0.03 . - No flow node ΔX = ΔY = 5 ft

Figure 12. Transmissivity map and model grid used in the USGS-2D saturated flow model.

bromide plume had moved past the wells. Diffuse recharge due to precipitation was neglected since it was insignificant during the testing period and it seemed unlikely that infiltration from the surface down thirty feet to the water table would be significant. As noted previously, the water table generally fell slightly during the study period.

The simulation was run as two separate pumping periods, as defined by Konikow and Bredehoeft (1978). The first pumping period included only the 24-hour injection interval at the start of the experiment. The injection flow rate was 2 gpm or 0.0045 cfs, at a concentration of 4350 mg/L. During the second pumping period, there was no injection or production of water. The second pumping period was set at six months in length since that duration included most of the meaningful bromide concentration fluctuations at wells A through J. The time steps used in the program were chosen small enough to avoid unsatisfactory behavior of the results, such as occasional negative concentrations near the plume boundary. As the numerical solution proceeded through time, the time step length was increased 20 percent between each step.

The remaining parameters which could be varied to affect the program results were transmissivities at the individual nodes, the longitudinal dispersivity (BETA in the program), the ratio of the transmissivities in the x- and y-directions (ANFCTR), and the ratio of the longitudinal and transverse dispersivities (DLTRAT). The major calibration checks were carried out by comparison of the concentration histories at wells D, E, G, and H to the model results. In addition, drilling logs for the wells served as reference information to support high or low local transmissivity values.

Model Results

As stated previously, modeling dispersive transport in alluvial aquifers is quite a challenge. As seen in the observed data (Figure 11), the bromide plume moved past well D toward wells E and H, yet the largest (over 170 mg/L) and sharpest observed concentration peak was observed at well G. The concentrations at wells E and H rose rather quickly, but remained elevated much longer than that at the other wells. These phenomena indicate that there must be a zone of high transmissivity between the injection well, (B) and Well G, while Wells E and H must be in a zone of low transmissivity which slowed the plume as it neared those wells. Over 100 combinations of transmissivity values and dispersivities were input to the program to attempt to simulate the observed conditions. Generally, it was difficult to obtain the high concentrations at Wells E and H without losing the sharp peak at Well G and vice versa. Since it was also impossible to set the Br concentrations at Wells A, C, and F to rise by more than 1 or 2 mg/L, so the calibration was based on the data from wells D, E, G, and H. In actuality, the final reported combination may not be the unique solution for this problem, but it provides a reasonable fit of the data and can be supported by evidence gathered during the well drilling process.

Figure 12 shows the transmissivity map which provided the closest fit of simulated concentrations to the observed data. As found by Davis (1986) and Chapelle (1986), manipulation of the nodal transmissivities was more effective than changing dispersivities to get reasonable fits. The transmissivity was set at $0.035 \text{ ft}^2/\text{s}$, which corresponds to a hydraulic conductivity of $750 \text{ gpd}/\text{ft}^2$, in most of the grid. This hydraulic conductivity is typical of that

seen in productive sections of the Ogallala in the Lubbock area. A small zone around Well D was given a smaller transmissivity of $0.002 \text{ ft}^2/\text{s}$ since there seemed to be resistance to flow between wells B and D which allowed only a small bromide concentration peak of approximately 50 mg/L. The well drilling log also indicated that the subsurface material in Well D was much tighter than Wells B and G. The zone east of Wells A and B and north of Well E was set at $0.01 \text{ ft}^2/\text{sec}$ ($215 \text{ gpd}/\text{ft}^2$) to encourage flow toward the northeast. The zone which includes Wells E and H was set at $0.00006 \text{ ft}^2/\text{sec}$ ($1.3 \text{ gpd}/\text{ft}^2$), which was required to slow the plume, yet still allow it to move to the north and east. The highest transmissivity value, $0.05 \text{ ft}^2/\text{sec}$ ($1080 \text{ gpd}/\text{ft}^2$), was needed near Well H to speed part of the plume toward that location. The zone around well J was set at $0.001 \text{ ft}^2/\text{sec}$ ($22 \text{ gpd}/\text{ft}^2$) to divert the plume toward the east and keep the peak concentration low at that location. The other transmissivity zones were also set by trial and error calibration to allow some needed transition zones between the other zones. Note that the range of transmissivity values in this small area is more than three orders of magnitude. It is possible in alluvial aquifers to have such discontinuities in hydraulic properties due to buried stream beds or clay plugs. The best value of the ratio of transmissivities in the x- and y-directions, the anisotropy factor, appeared to be 1.0, as small increases in either direction combined with the northeasterly hydraulic gradient to move the plume either only to the north or only to the east.

In addition to controlling the plume movement, the transmissivity distribution also affected the head distribution within the study area. Table 2 shows a comparison of the average and simulated water table elevations at Wells A through J. The simulated values were within 0.1 ft of the average measured data for 8 of the 9 wells included in the simulation. The actual water table elevations did tend to slowly decrease over the study period, but the USGS-2D model does not include a mechanism to accurately simulate that situation. Since the water levels in all the wells fell relatively uniformly, it seemed reasonable to model the average condition for the study period. The actual concentration histories at Wells D, E, G, and H are compared to the best simulation results as shown in Figures 13 through 16. The longitudinal dispersivity was set at 2.5 ft, and the ratio of transverse to longitudinal dispersivity was 0.3. At all four wells, it was possible to exactly simulate the initial breakthrough of the Br plume and still approximate the peak concentration and the duration of the elevated concentration. The simulation at Well G is obviously the closest to the actual data, with the peak concentration and time to peak approximated well. The simulation at Well D approximated the peak concentration well, but the simulated concentration history lags behind the actual data by about 20 days. At Well E, the simulated concentrations rise almost as quickly as the actual concentrations and the peak concentration is matched fairly well. However, the simulated concentration falls off much sooner than the actual data. At Well H, the simulated concentration rises about 30 days later than the actual data, approximates the peak concentration well, then decreases earlier than the actual data. Attempts to modify the longitudinal dispersivity or ratio of longitudinal to transverse dispersivity to spread the plume resulted in lower peak concentrations at Wells E, G, and H while increasing the peak concentration at Well D. Even though the overall match between the simulated and actual results is not perfect, the general trends of the simulation results are correct and can be used to interpret the properties of the aquifer.

Table 2. Average and Simulated Water Table Elevations.

Well	Average Elevation (ft)	Range	Simulated Elevation (ft)
A	3195.4	3194.8 - 3195.7	3195.39
B	3195.1	3194.7 - 3195.6	3195.31
C	3195.3	3193.5 - 3195.6	3195.20
D	3195.2	3194.8 - 3195.5	3195.18
E	3195.2	3193.6 - 3195.6	3195.14
F	3195.2	3194.1 - 3195.4	3195.05
G	3195.2	3194.8 - 3195.4	3195.06
H	3194.1	3194.4 - 3195.4	3195.07
J	3194.9	3194.4 - 3195.3	3194.61

A second comparison of the model results to the actual field data was made by inspection of the contours of equal Br concentration. The field data provided roughly simultaneous observations at ten locations within the study area. The model required much finer discretization of the study area, as discussed previously, and generated concentration values for all nodes in the grid. Thus, contours for the actual data were generated from a much sparser data set than those calculated by the model, and strict agreement between actual and model contours at similar time steps is not insured. Still, it is possible to evaluate the results in a somewhat qualitative sense. Figures 17 through 20 show the actual and model contours derived by a commercial plotting program at times 50, 75, 100, and 185 days after injection. These dates were chosen to typify the general plume movement. Similar trends in the contours for both the modeled and field data were apparent, as the peak of the plume passed Well G after 50 days then dissipated eastward rather than migrating toward Well J. The model and actual contours compare quite well after 50 days, but the agreement deteriorates as time increases, similar to the comparisons in Figures 13 to 16. Figures 17 to 20 demonstrate the best-fitting model results that were possible with this application of the model, and though slightly imperfect, the comparison does show that the heterogeneous effects can be represented within the model.

The results of the USGS-2D model effort must be viewed with recognition of the limitations of the model. First, the model only allows variation of transmissivity in the two-dimensional horizontal plane. The subsurface at the test site was found to have significant vertical interbedding of layers of differing materials. If these layers affect the flow, as they likely did in this case, the model is not able to represent them. A second limitation of the model is that it only allows a single value of anisotropy factor, the ratio of transmissivity in the x- and y-directions, for the entire model grid. Certainly, in alluvial deposits such as the Ogallala, hydraulic anisotropy can

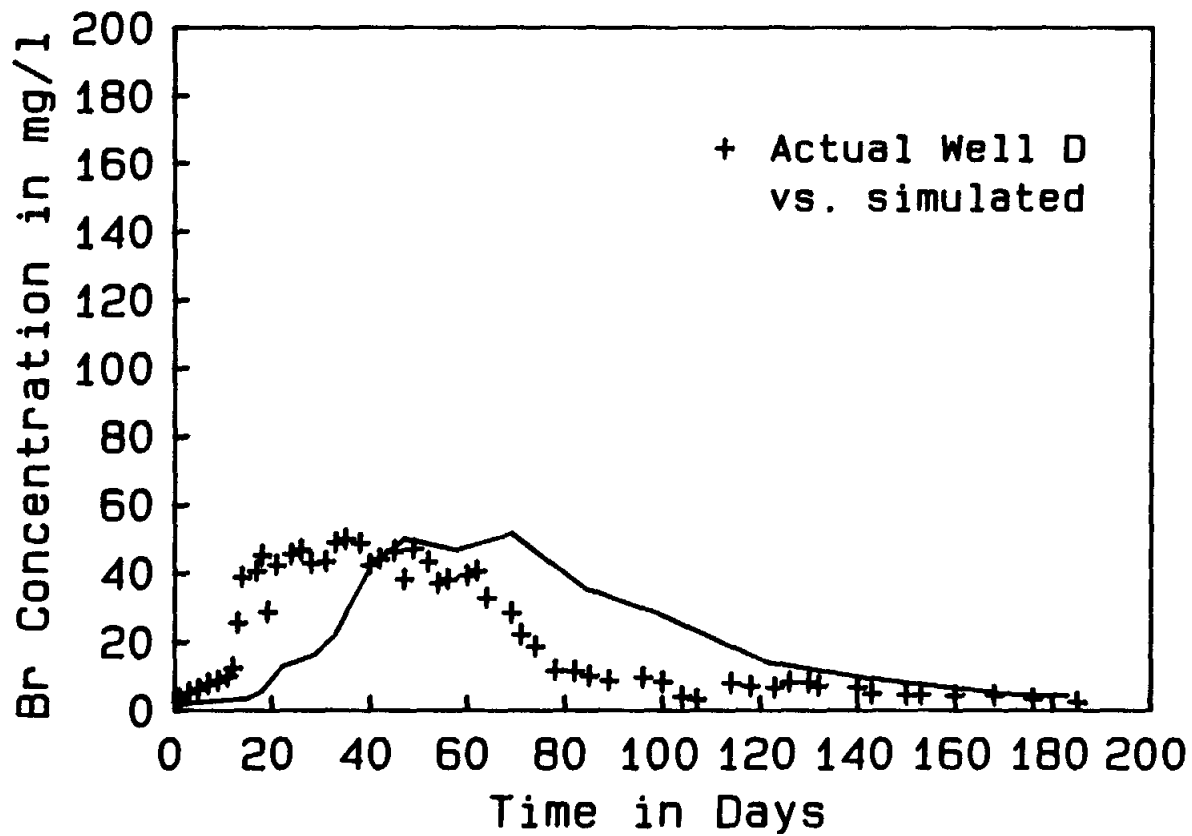


Figure 13. Bromide concentration history for actual and simulated data for Well D.

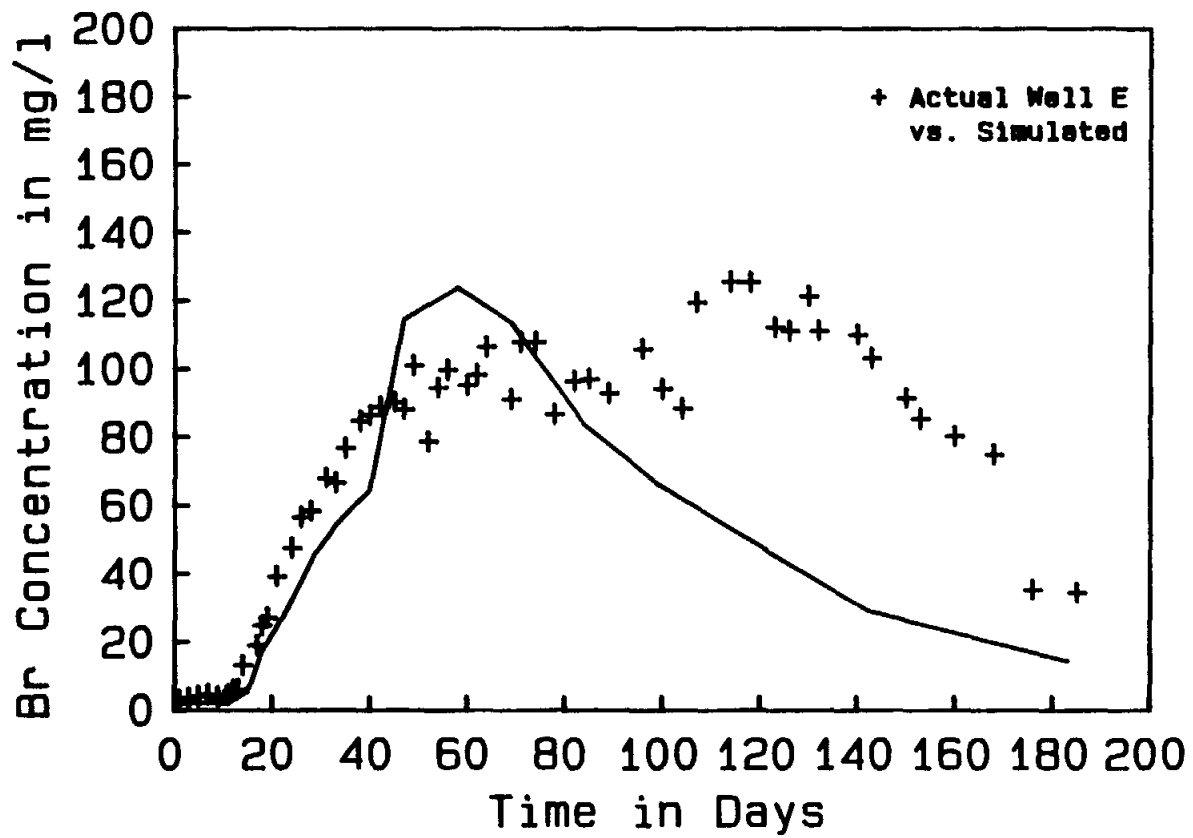


Figure 14. Bromide concentration history for actual and simulated data for Well E.

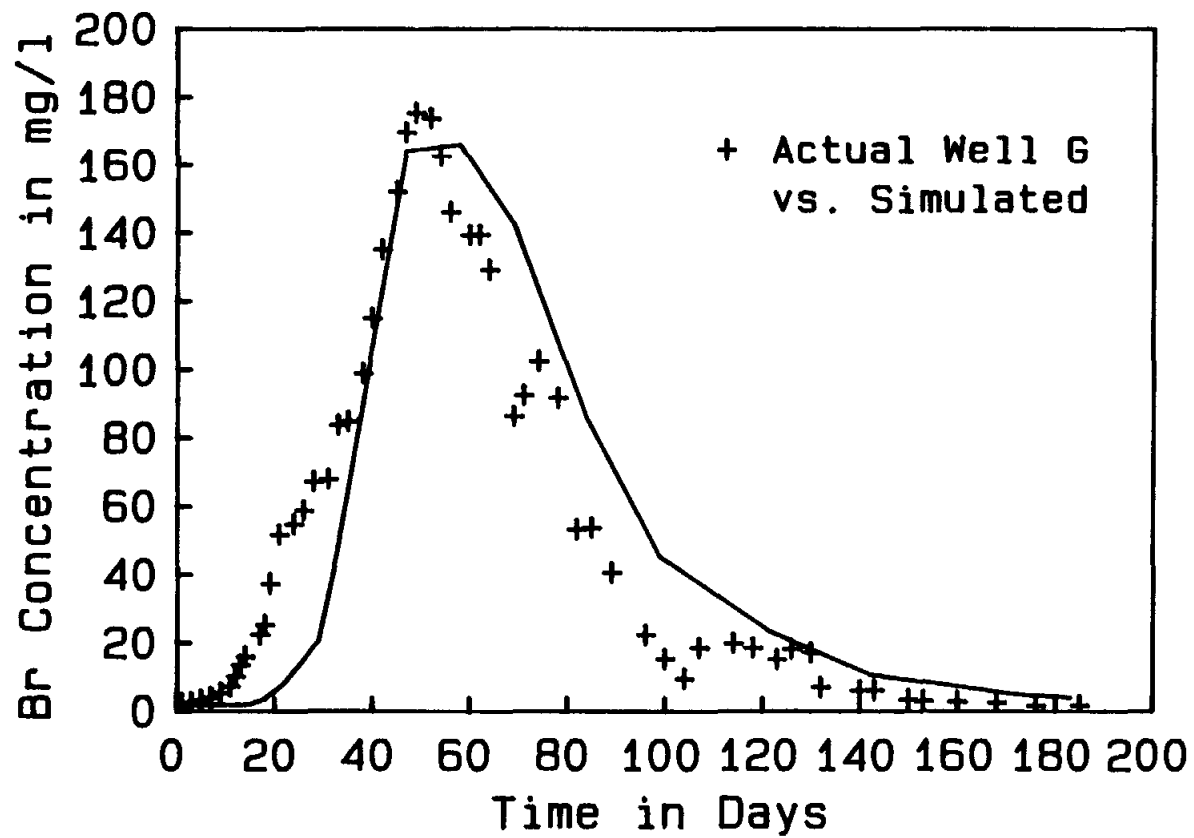


Figure 15. Bromide concentration history for actual and simulated data for Well G.

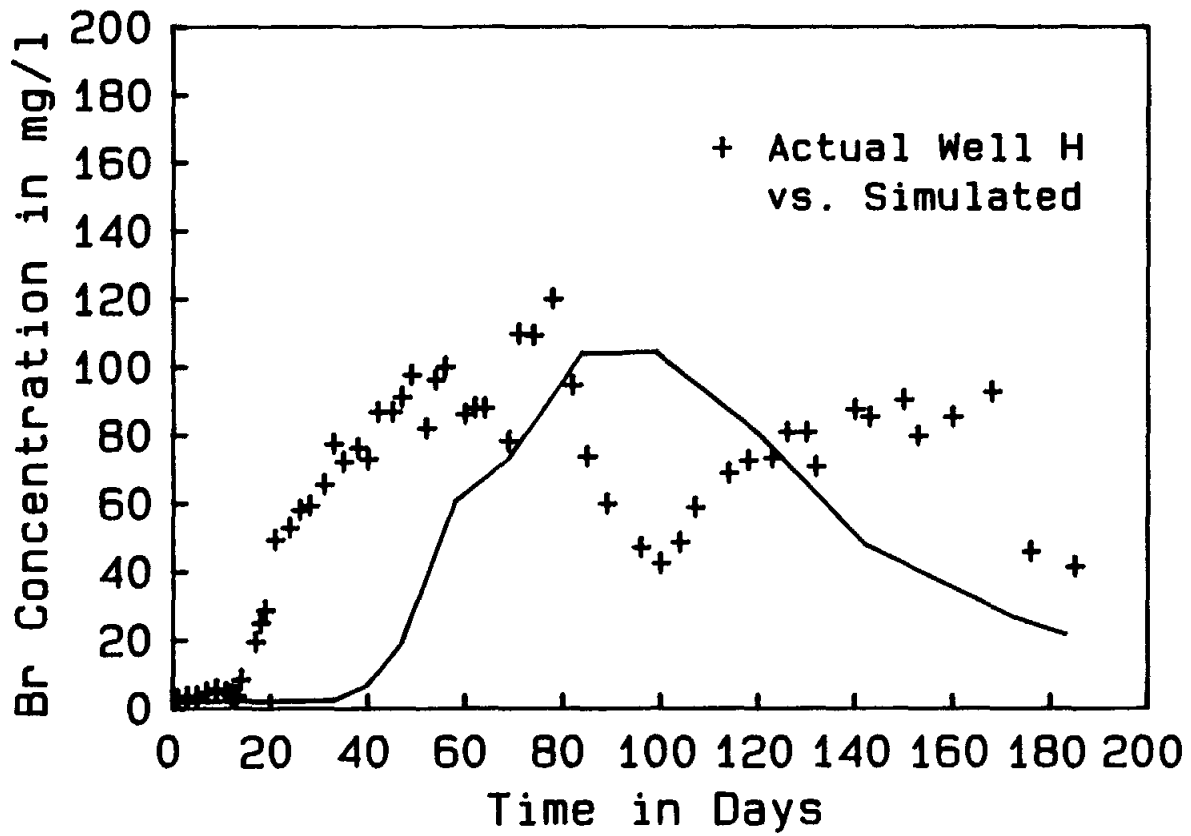


Figure 16. Bromide concentration history for actual and simulated data for Well H.

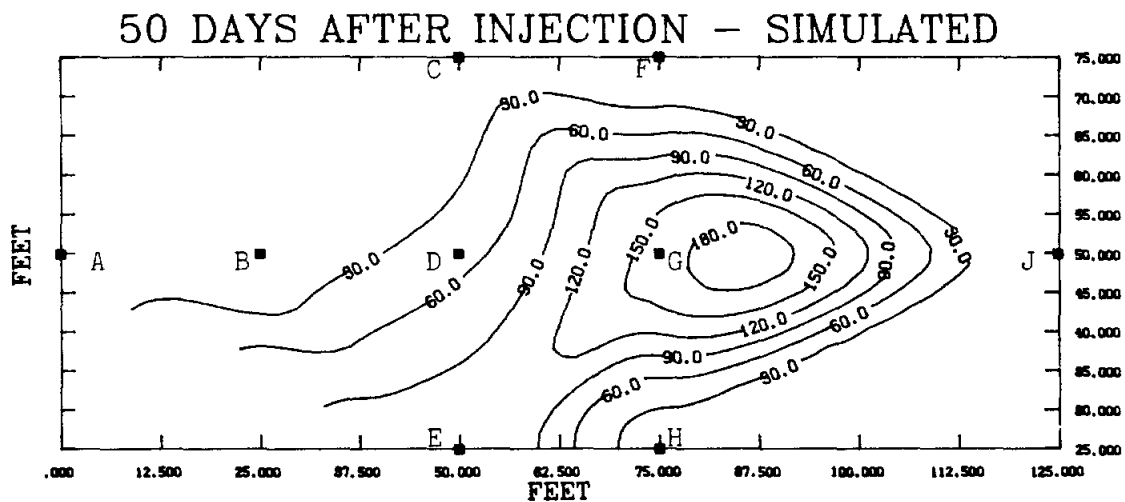
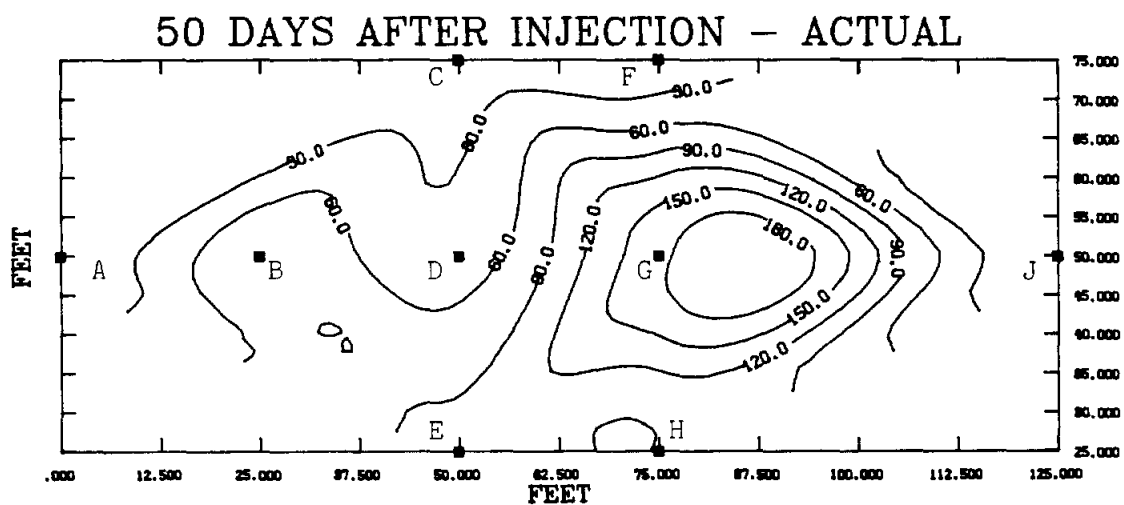


Figure 17. Bromide concentration contours for actual and simulated data for day 50 following tracer injection.

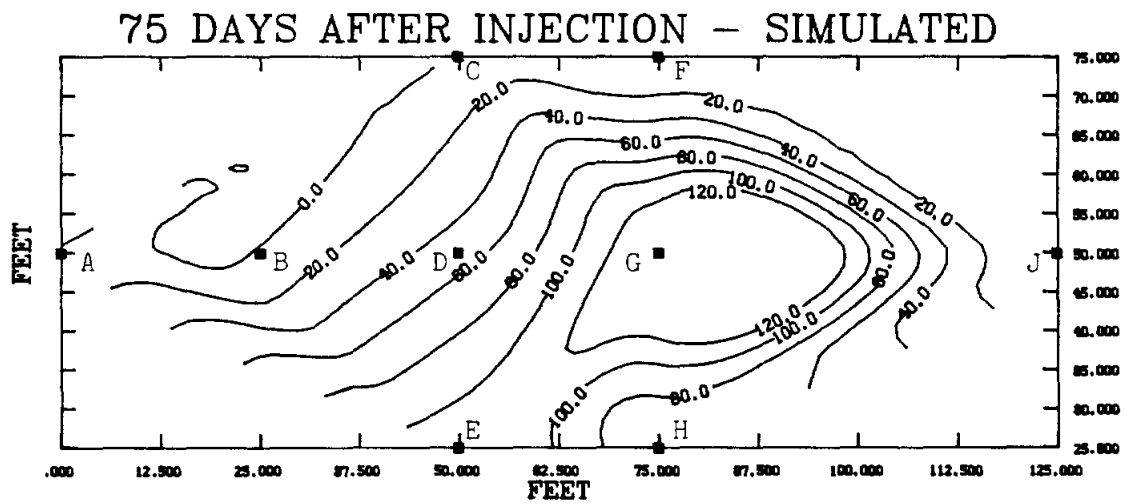
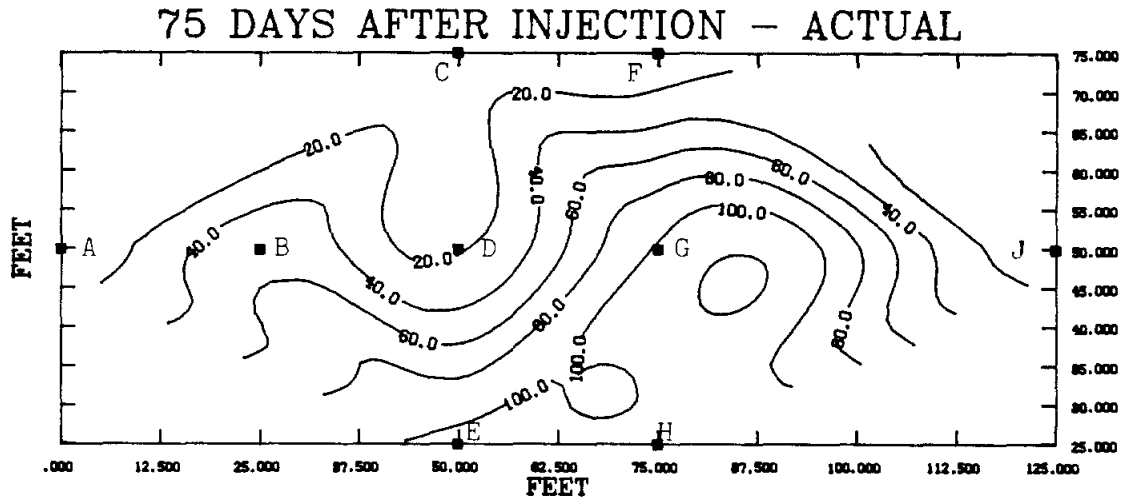


Figure 18. Bromide concentration contours for actual and simulated data for day 75 following tracer injection.

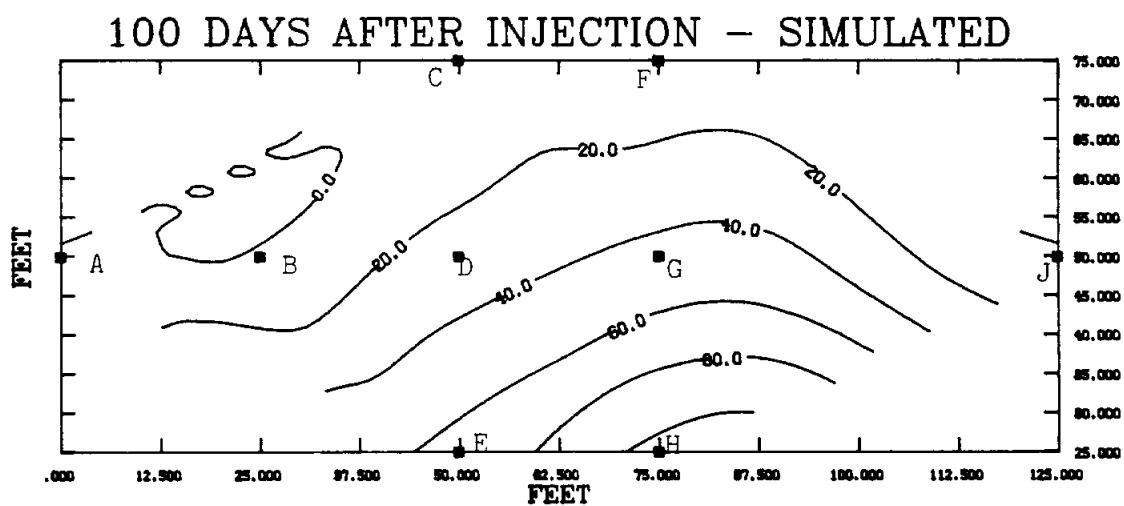
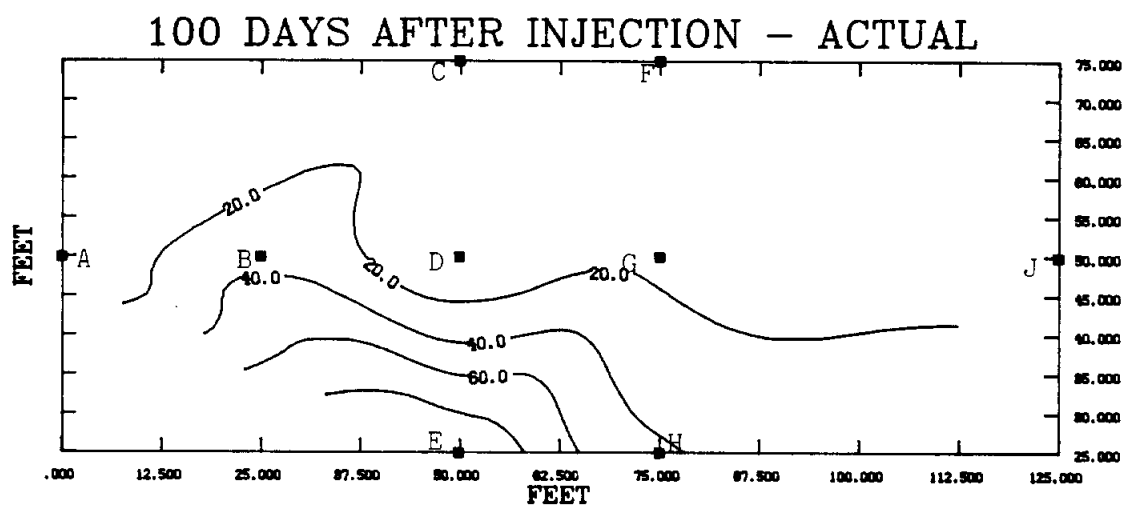


Figure 19. Bromide concentration contours for actual and simulated data for day 100 following tracer injection.

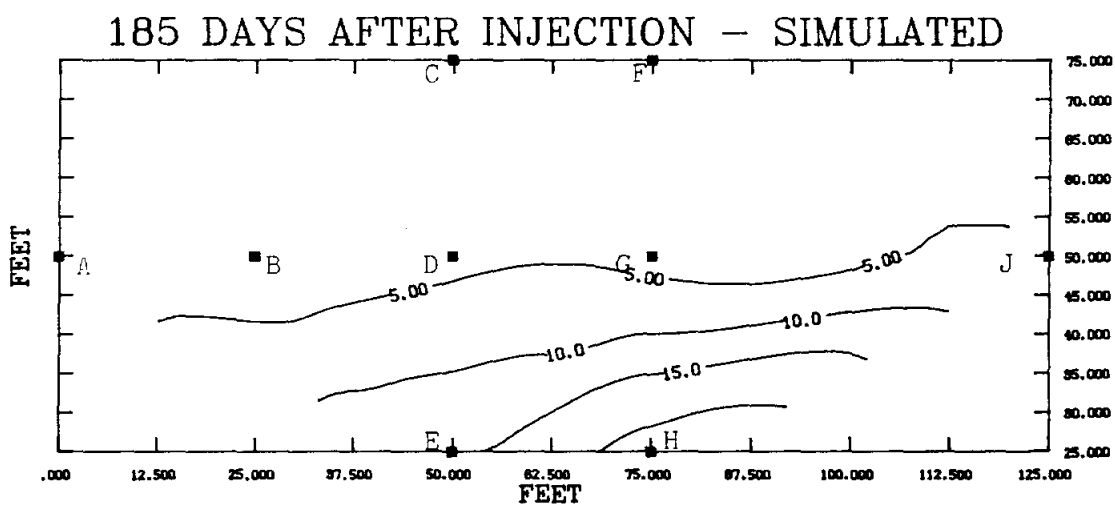
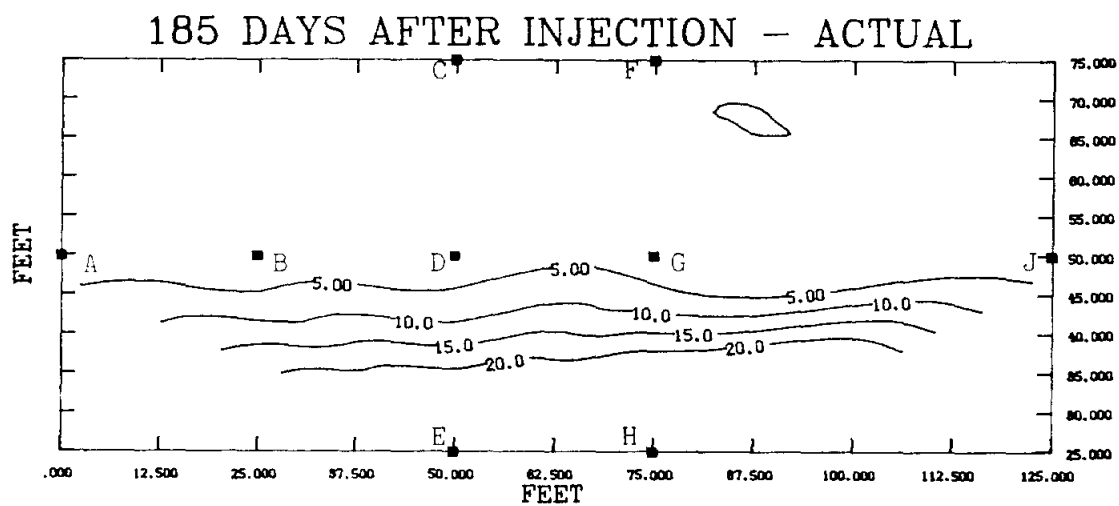


Figure 20. Bromide concentration contours for actual and simulated data for day 185 following tracer injection.

vary from place to place due to the depositional history of the various materials. Third, as in any numerical model, the value of concentration at a node is actually the average value for the $\Delta x \Delta y$ area surrounding that node. This can lead to inaccuracies in the estimated concentrations at any point in the grid system. Fourth, the fineness of the grid system used to discretize the study area limits the amount of model "fine-tuning" the modeler may do during calibration. As the grid gets finer, which may allow greater accuracy of simulation, the model input data becomes more cumbersome to manipulate and the computer processing time increases dramatically. In this project, the USGS-2D model was intended to help the research team estimate the variability of the hydraulic parameters of a small section of the Ogallala and examine the effects on the movement of solutes in the groundwater. The model was useful for this purpose.

Discussion of Modeling Efforts

The primary purpose of this part of the project was to observe the movement of a tracer in the Ogallala aquifer. The modeling of the observed data indicate that although the hydraulic gradient does affect flow, local transmissivity zones can also affect the speed and spreading of a solute plume. Contaminant plumes in this type of aquifer will not easily spread and dilute as in a more homogeneous aquifer. The USGS-2D model was useful in describing the possible geologic conditions which could explain the observed plume movement in this study. Even with limited actual sample information from the subsurface, the computer model can supplement that evidence to broaden the understanding of the solute transport process.

Other conclusions from this modeling effort must acknowledge some limitations of the study. Any research project is limited by the time and finances available, and subsurface investigations are also affected by the many assumptions that must be made based on limited data. In this study, the local water table fluctuation due to infiltration or other areal effects were neglected. Only small variations in the water table elevations, on the order of tenths of feet, were noted during the study period, so average values were used in the model. In the small study area, however, even small differential changes could cause temporary reversals in flow directions. The model allows specification of various hydraulic parameters at each node, but it could be that subsurface channeling and clay lenses could cause non-Darcian flow. Small regions of high permeability could have sped the flow from Well B to Well G, while a different flow regime could exist between Well B and Well E. It is impossible to establish the configuration of the subsurface with perfect accuracy, with or without a computer model. Even though this was a small-scale field test, it is possible that still more geologic data is required to allow accurate modeling. The project budget allowed for the drilling of small holes typically used for monitor wells as well as the installation of the wells.

CONCLUSIONS AND RECOMMENDATIONS

The primary purpose of this study was to observe the movement of a pollutant in the environment and conduct a field study of the potential movement of the pollutant if it were to enter the groundwater in the Texas High Plains. It was determined that the concentrations of agricultural pesticides applied to the soil surface were not large enough to move directly toward the

groundwater and become a nuisance. Therefore, the potential movement of a chemical from the surface to sedimentation areas via the erosion transport mechanism were examined.

Natural movement of the chemical Trifluralin was found to occur due to erosion but the field samples collected were not significantly different than the occurrence from a previous year's residual level. A test of chemical movement specifically by wind was conducted in a controlled wind tunnel. The results showed that some chemical, when adsorbed to soil particles, would be transported from one location to another with the soil. The deposition areas for this transported soil are generally low-lying areas that collect runoff from a storm event. An example of a collection area in the Texas High Plains are playa lakes. The result of soil/chemical deposition simulated to be an increase in chemical concentration. These soil deposition areas begin to develop a point where the chemical may develop a path toward groundwater. The concentration of chemical transported by wind was nearly doubled for the case where some surface cover was available as compared to a bare soil surface, but the total quantity of chemical transported was reduced. Concentration increases are acceptable because the total surface area to which the chemical was attached increases for the surface cover condition when only the smaller sized soil particles were moved compared to all sizes of particles being transported. Modeling efforts proved the near doubling in chemical concentration for the surface cover condition was accurate when the assumption of a uniform soil particle distribution is made. For the sieved soil used in the tests, the assumption is valid.

Unsaturated flow simulations proved that under homogeneous conditions, a chemical applied to the soil surface will travel approximately 4 feet vertically and 3 feet horizontally after 60 days provided there was a continuous application of the chemical. This proves that the pathway of a surface applied chemical is not through a soil profile as explained by a Darcian flow condition but by another direct pathway, such as a well or macropore.

The modeling of the observed groundwater flow data indicate that although the hydraulic gradient does affect flow, local transmissivity zones can also affect the speed and spreading of a solute plume. Contaminant plumes in this type of aquifer will not easily spread and dilute as in a more homogeneous aquifer. The USGS-2D model was useful in describing the possible geologic conditions that explain the observed plume movement in this study.

A major conclusion made from the tracer test results is that the movement of solutes in groundwater in this section of the Ogallala is difficult to predict. Subsurface descriptions from the examination of drilled materials were helpful in identifying possible zones of different permeability, but these data are limited by the small number of discrete point locations within the site. When the solute is within a relatively permeable zone, it may vary at velocities which change by one order of magnitude. Pollutants could be very mobile in this situation and the more permeable zones cannot be located easily from the surface. On the other hand, when the solute reaches a zone of dense materials, it may remain there at relatively high concentrations for a significant period of time. Removal of groundwater pollutants from such a low permeable zone would be more difficult than from a zone in which the permeability is high. Both these situations are important considerations for

protection and restoration of local groundwater quality. Since the Ogallala is an important water resource for the Texas High Plains, any pollutant which enters the aquifer from human sources could be very difficult to track or remove.

Other conclusions from this modeling effort must acknowledge the limitations of the study. Any research project is limited by the time and finances available, and subsurface investigations are also affected by the numerous assumptions that must be made based on limited data. In this study, the local water table fluctuation due to infiltration or other areal effects was negligible. Only small variations in the water table elevations, on the order of tenths of feet, were noted during the study period, so average values were used in the model. The model allows specification of various hydraulic parameters at each node, but it could be that subsurface channeling and clay lenses could cause non-Darcian flow. Small regions of high permeability could have increased the solute flow from Well B to Well G, while a different flow regime could exist between Well B and Well E. It is impossible to establish the configuration of the subsurface with perfect accuracy, with or without a computer model. Even though this was a small-scale field test, it is possible that still more geologic data is required to allow accurate modeling. This project was restricted to the drilling of small holes typically used for monitor wells and the installation of wells.

It is recommended that additional wind tunnel studies be performed so model calibration can be made for several soil types and the possibility of developing a single general model for chemical transport caused by wind erosion. Further model identification will allow the model to be used to simulate different cropping systems for the benefit of reducing soil and/or pesticide movement.

Since the soil profile contains marked stratification due to alluvial deposits, a large scale field study to examine the effects of stratification on solute movement should be made. Unfortunately, this type of study would be expensive due to the very large numbers of test wells that would be required. Also, core samples of the soil strata would be needed and this would require specialized equipment.

In addition, three dimensional (3-D) field study of an aquifer would provide much insight to solute movement across the entire saturated thickness. The 3-D studies would be helpful in studying the effects of dilution that occurs naturally in an aquifer. Again, this type of study would be very expensive, time consuming and risky, but it could provide insight to the large scale movement of a solute in groundwater aquifers.

REFERENCES

- Acharya, B. P. 1986. A finite difference model for flow of a pollutant through unsaturated porous media. M.S. Thesis, Texas Tech University, Lubbock, TX.
- American Public Health Association. 1985. Standard methods for the examination of water and wastewater. 16th ed. New York, NY 10019.
- Brantly, J.E. 1961., Rotary drilling handbook, (6th Ed.): New York, Palmer Publications, 825p.
- Carter, D.L. and J.A. Bondurant. 1976. Control of sediments, nutrients, and adsorbed biocides in surface irrigation return flows. Report No. EPA-600/2-76-237. Ada, OK.
- CAST. 1985. Agricultural and groundwater quality. Report No. 103 Council for Agricultural Science and Technology., Ames, IA 50010.
- Chapelle, F.H. 1986. A solution-transport simulation of brackish water intrusion near Baltimore, Maryland, Groundwater, 24(3).
- Chen, Y. C. 1987. Economic potential for development of increasing groundwater storage beneath a High Plains municipality. M.S. thesis, Texas Tech University, Lubbock, TX.
- Cheng, H.H. and W. C. Koskinen. 1986. Processes and factors affecting transport of pesticide to ground water. In: Evaluation of Pesticides in Ground Water. American Chemical Society, Washington, D.C.
- Davis, A.D. 1986. Deterministic modeling of dispersion in heterogeneous permeable media, Groundwater, 24(5).
- Davis, S.N., G.M. Thompson, H.W. Bentley and G. Stiles. 1980. Ground-water tracers--A short review, Groundwater, 18(1), 14-23.
- Driscoll, F.G. 1986. Groundwater and Wells, 2nd ed., Johnson Division, St. Paul, MN 55112.
- Gregory, J.M. and J. Borrelli. 1986. The Texas Tech Wind Erosion Equation. ASAE Paper No. 86-2528. St. Joseph, MI 49085.
- Gregory, J.M., C.B. Fedler and J. Borrelli. 1988. TEAM - Texas Erosion Analysis Model. Paper No. 88-2121 presented at the Summer Meeting of the ASAE, Rapid City, SD. June.
- Haith, D.A. 1980. A mathematical model for estimating pesticide losses in runoff. J. Environ. Qual. Vol. 9(3):428-433.
- Hillel, D. 1980. Fundamentals of Soil Physics. Academic Press Inc., 111 Fifth Ave., New York, NY 10003.

Konikow, L.F., and J.D. Bredehoeft. 1978. Computer model of two-dimensional solute transport and dispersion in ground water. Chapter C2, Techniques of Water--Resources Investigations of the U.S. Geological Survey. Book 7: U.S.G.S., Reston, Virginia.

Lee, G.F., and R.A. Jones. 1983. Guidelines for sampling ground water, J. WPCF, 55(1), 92-96, Jan.

Leonard, R.A., G.W. Langdale and W.G. Fleming. 1979. Herbicide runoff of Upland Piedmont watersheds--data and implications for modeling pesticide and transport. J. Environ. Qual. Vol. 8(2): 223-229.

Maulem, Y. 1976. A catalogue of the hydraulic properties of unsaturated soils. Development of methods, tools and solutions for unsaturated flow with application to watershed hydrology and other fluids. Hafia, Israel.

Mulkey, L.A., R.F. Corsel, and C.N. Smith. 1986. Development, testing and applications of nonpoint source models for evaluation of pesticide risk to the environment. In: Agricultural Nonpoint Source Pollution: Model Selection and Application. eds. A giorgini and F. Zingales. Elvsevien Science Pub. B.V. New York. pps 383-397.

Nicholson, H.P., A.R. Grzenda, G.L. Louer, W.S. Cox, and J.I. Teasley. 1964. Water pollution by insecticides in an agricultural river basin: occurrence of insecticides in reiver and treated municipal water. Limol. and Oceanogr. 9:310-317.

Ristau, R.J. 1982. Herbicide loss due to irrigation of runoff on cropland -- A Literature Review. Dept. Environmental Quality, Water Quality Division, Cheyenne, Wyoming 82002.

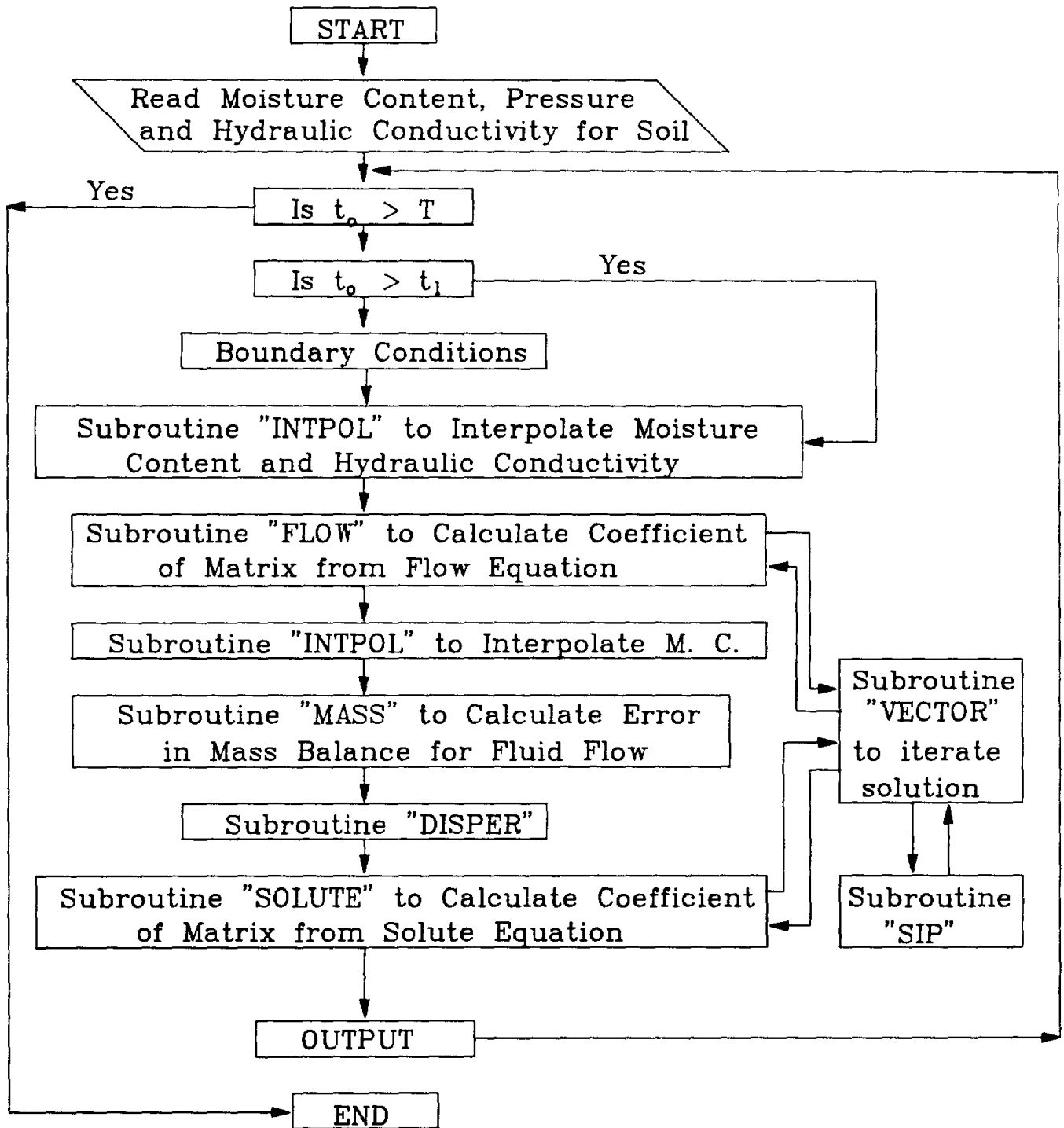
Triplett Jr., G.B., B.J. Conner and W.M. Edwards. 1978. Transport of atrazine in runoff from conventional and no-tillage corn. J. Environ. Qual. Vol. 7(1): 77-84.

Wauchope, R.D. 1978. The pesticide content of surface water draining from agricultural fields - A review. J. Environ. Qual. Vol. 7 (4): 459-472.

Zison, S.W. 1980. Sediment-pollutant relationships in runoff from selected agricultural, suburban and urban watersheds. Report No. EPA-600/3-80-022. Athens, Georgia.

APPENDIX A

**Flow diagram and listing of the
2-D Unsaturated flow model program**



```

1 C *****
2 C *
3 C *          MAIN PROGRAM          *
4 C *
5 C *          FOR                    *
6 C *
7 C *    TRANSPORTATION OF SOLUTE THROUGH POROUS MEDIA *
8 C *
9 C *          BY                      *
10 C *
11 C *    B.P. ACHARYA, S.B. BELKNAP, C.B. FEDLER *
12 C *
13 C *****
14 *$NLIST
15     IMPLICIT REAL *8(A-H,O-Z)
16     DIMENSION SL1(11,11),SL2(11,11),FMC(21),P(21),PERM(21)
17     CHARACTER*14 FILENM,OUTFL
18 3   CHARACTER*25 SOILTP
19     COMMON /CON/ C(11,11)
20     COMMON /PH/ HC(11,11),PHI(11,11)
21     COMMON /ACCLP/ K2,KOUNT,W(4)
22     COMMON /MBAL/ WW,SLWC(1,11)
23     COMMON /WATER/ WCON(11,11)
24     COMMON /SID/ VX(11,11),VZ(11,11),DISX(11,11),DISZ(11,11)
25     COMMON /CONST/ M,N,T,T1,JJ
26 C     HC = HYDRAULIC CONDUCTIVITY (FT/HR)
27 C     PHI = PRESSURE AT EACH NODE AT TIME (FT)
28 C     SL1 = SLOPE OF PRESSURE AND MOISTURE CURVE
29 C     C = SOLUTE CONCENTRATION
30 C     VX = VELOCITY COMPONENT ALONG X DIRECTION
31 C     VZ = VELOCITY COMPONENT ALONG Z DIRECTION
32 C     DISX= DISPERSION CO-EFFICIENT ALONG X DIRECTION
33 C     DISZ= DISPERSION CO-EFFICIENT ALONG Z DIRECTION
34 C     W = ACCELERATION PARAMETER FOR STRONGLY IMPLICIT SCHEME
35 C     N = NUMBER OF NODES ALONG X DIRECTION
36 C     M = NUMBER OF NODES ALONG Z DIRECTION
37 C     DX = INCREMENTAL LENGTH ALONG X DIRECTION
38 C     DZ = INCREMENTAL LENGTH ALONG Z DIRECTION
39 C     DT = TIME INCREMENT
40 C     PSMC= SATURATION MOISTURE CONTENT
41 C     PSAT= PRESSURE CORRESPONDING TO SATURATION M.C.
42 C     DISL= LONGITUDINAL DISPERSIVITY IN FT**2/HR.
43 C     RATIO = RATIO OF TRANSVERSE TO LONGITUDINAL DISPERSIVITY
44 C     TDIS= TRANSVERSE DISPERSIVITY
45 C     Z =DEPTH OF UNSATURATED SOIL
46 C     X1 = DISTANCE ALONG X DIRECTION UP TO WATER IS APPLIED
47 C     FC = INITIAL SOIL MOISTURE CONTENT
48 C     AK = ACCELERATION PARAMETERS
49 C     T1 = TIME UNTIL WATER IS APPLIED AT THE SURFACE
50 C     CO = CONCENTRATION OF THE SOLUTE APPLIED
51 C     LTST= LENGTH OF TOTAL SIMULATED TIME
52 C     FACTOR = CONVERSION FACTOR TO CONVERT HYDRAULIC CONDUCTIVITY
53 C             IN SQ.FT. TO FT./HR.
54 C     P = PRESSURE FROM TABLE
55 C     FMC = MOISTURE CONTENT FROM TABLE

```

```

56 C      WCON= INTERPOLATED MOISTURE CONTENT
57 C      SLWC= WATER CONTENT OF THE SURFACE LAYER UNTIL TIME T1
58 C      LK = KK = NUMBER OF DATA POINTS ON PRESSURE MOISTURE CURVE
59 C      FILENM = FILE NAMES
60 C      SOILTYP = THE NAME OF THE SOIL TYPE IN THE SOIL FILE
61 C
62 C
63      DATA DISL /0.00462667/,RATIO /0.3/
64      DATA FACTOR /1.29168E+11/
65      WRITE(*, '(1X,A)\') 'ENTER THE DATA FILE NAME '
66      READ (*, '(A)') FILENM
67      OPEN (6, FILE = FILENM, STATUS='OLD')
68      READ (6, *) DX
69      READ (6, *) DZ
70      READ (6, *) DT
71      READ (6, *) Z
72      READ (6, *) X
73      READ (6, *) LTST
74      READ (6, *) TOLER
75      READ (6, *) X1
76      READ (6, *) T1
77      READ (6, *) FC
78      READ (6, *) CO
79      READ (6, *) TIME
80      CLOSE(6)
81
82 *
83      IF (TIME .GE. 0.04 .AND. TIME .LE. 0.05) THEN
84          DAYUN = ' DAY'
85      ELSEIF (TIME .GE. 0.9 .AND. TIME .LE. 1.1) THEN
86          DAYUN = ' HOUR'
87      ELSEIF (TIME .GE. 59.0 .AND. TIME .LE. 61.0) THEN
88          DAYUN = ' MINUTE'
89      END IF
90 *
91      FACTOR=(FACTOR)/(12.*TIME)
92      N=X/DX+1
93      M=Z/DZ+1
94      DO 2 I=1, M
95          DO 3 J=1, N
96              PHI(I, J)=0.0
97              HC(I, J)=0.0
98              SL1(I, J)=0.0
99              SL2(I, J)=0.0
100             C(I, J)=0.0
101             WCON(I, J)=0.0
102             VX(I, J)=0.0
103             VZ(I, J)=0.0
104             DISX(I, J)=0.0
105             DISZ(I, J)=0.0
106 3      CONTINUE

```

```

107 2      CONTINUE
108      JJ=(X1/DX)+1
109      WRITE (*,'(A)') ' ENTER FILE WITH SOIL TYPE '
110      READ (*,'(A)') FILENM
111      OPEN(7,FILE=FILENM,STATUS='OLD',ACCESS='SEQUENTIAL',
112 1      FORM='FORMATTED')
113      READ(7,'(A)') SOILTP
114      READ(7,100) FSMC,(PERM(I),P(I),I=1,21)
115      WRITE (*,'(A)') ' USE "OUTPUT1" AS DEFAULT OUTPUT FILE OR ENTER '
116      WRITE (*,'(A)') ' A NEW FILE NAME <"D"efault/"N"ew> '
117      READ (*,'(A)') ANS
118      IF (ANS .EQ. 'd' .OR. ANS .EQ. 'D') THEN
119          OUTFL = 'OUTPUT1'
120      ELSE
121          WRITE (*,'(A)') ' ENTER A NEW FILE NAME '
122          READ (*,'(A)') OUTFL
123      END IF
124 *
125 *      SET THE SKIP IN PRINTOUT
126 *
127      WRITE (*,'(A)') ' ENTER THE NUMBER OF TIME PERIODS TO SKIP IN THE
128 1OUTPUT FILE'
129      READ (*,*) INSKIP
130      ISKIP = 0
131      OPEN(9,FILE=OUTFL,STATUS='NEW',ACCESS='SEQUENTIAL',
132 1      FORM='FORMATTED')
133      POR = FSMC
134      PSMC = FSMC
135      PSAT = P(21)
136      WRITE(9,101) SOILTP
137      WRITE(9,102)
138      WRITE(9,103)DX
139      WRITE(9,104)DZ
140      WRITE(9,106)DT
141      WRITE(9,109)
142      WRITE(9,107)FC
143      WRITE(9,202)CO
144      WRITE(9,108)POR
145      WRITE(9,110)LTST,DAYUN
146      WRITE(9,111)T1,DAYUN
147      WRITE(9,201)TOLER
148      DISL=DISL/TIME
149      SMC=100.*FC
150      T=0.0
151 C
152 C
153 C      -----
154 C      - INITIAL CONDITIONS -
155 C      -----
156      FMC(1)=0.0
157      LK=21

```

```

158     PSAT=P(LK)
159     DO 10 KK=2,LK
160         FMC(KK)=FMC(KK-1)+0.05
161 10    CONTINUE
162     MCON=LK
163     DO 13 I=1,M
164         DO 12 J=1,N
165             IF(I.GT.1)GO TO 11
166             IF(J.GT.JJ)GO TO 11
167             WCON(I,J)=FMC(MCON)
168             C(I,J)=C0
169             GO TO 12
170 11    WCON(I,J)=FC
171         C(I,J)=0.0
172     CONTINUE
173 13    CONTINUE
174 C
175     CALL INTPOL (WCON,PHI,SL1,FMC,P,LK,PSMC)
176 C
177 C
178 C     COMPUTATION OF MAXIMUM VALUE OF ACCELERATION PARAMETER
179 C
180 C
181     AW1=((DX/X)**2.)
182     AW2=((DZ/Z)**2.)
183     AW3=(2.*AW1)/(1.+(AW1/AW2))
184     AW4=(2.*AW2)/(1.+(AW1/AW2))
185     AW5=AW3-AW4
186     IF(AW5.GE.0.0)THEN
187         WMAX=1-AW4
188     ELSE
189         WMAX=1-AW3
190     ENDIF
191 C
192 C     COMPUTATION OF ACCELERATION PARAMETERS
193 C
194 C
195     MA=4
196     W(1)=0.0
197     DO 50 MM=2,MA
198         AM=(DBLE(MM-1))/(DBLE(MA-1))
199         W(MM)=1.0-((1.0-WMAX)**AM)
200 50    CONTINUE
201     NI=0
202     WW=(M-1)*(N-1)*FC*(DX*DZ*POR)
203     VOL=DX*DZ*POR
204     NIT=LTST/DT
205     DO 1 I2=1,NIT
206         NI=NI+1
207         WRITE(*,112)NI
208     T=T+DT

```

```

209 C
210 C      CALCULATION FOR FIRST TIME STEP WITH INITIAL CONDITIONS
211 C      -----
212 C
213 C      IF(T.LE.DT) GO TO 53
214 C      IF(T.GT.T1) GO TO 54
215 C      DO 52 J=1,M
216 C      DO 51 I=1,N
217 C      IF(I.EQ.1.AND.J.LE.JJ) THEN
218 C      PHI(I,J)=PSAT
219 C      C(I,J)=C0
220 C      ELSE
221 C      ENDIF
222 51 CONTINUE
223 52 CONTINUE
224 53 CONTINUE
225 C
226 C      CALL INTPOL (PHI,WCON,SL1,P,FMC,LK,PSAT)
227 C      -----
228 C
229 54 CALL INTPOL (WCON,HC,SL2,FMC,PERM,LK,PSMC)
230 C      -----
231 C
232 C      DO 56 I=1,M
233 C      DO 55 J=1,N
234 C      HC(I,J)=HC(I,J)*FACTOR
235 55 CONTINUE
236 56 CONTINUE
237 C      DO 57 J=1,M
238 C      SLWC(1,J)=WCON(1,J)
239 57 CONTINUE
240 C      SAT=PSAT
241 C
242 C      CALL FLOW (DX,DZ,DT,SL1,TOLER,SAT)
243 C      -----
244 C
245 C      CALL INTPOL (PHI,WCON,SL1,P,FMC,LK,PSAT)
246 C      -----
247 C
248 C      IF(T.LE.T1)GO TO 58
249 C
250 C      CALL MASS (VOL,EROR)
251 C      -----
252 C
253 *
254 *      SET UP SKIP IN THE PRINT OUT
255 *
256 58 IFSKIP = 0
257 ISKIP = ISKIP + 1
258 IF (INSKIP .EQ. ISKIP) THEN
259 ISKIP = INSKIP - ISKIP

```

```

260     IFSKIP = 1
261     ELSE
262     GO TO 60
263     END IF
264 *
265     WRITE(9,109)
266     WRITE(9,113)T, DAYUN
267     WRITE(9,114)
268     WRITE(9,109)
269     WRITE(9,115)
270     WRITE(9,116)
271     DO 59 J=1,11
272     WRITE(9,117)J,WCON(1,J),WCON(2,J),WCON(3,J),WCON(4,J),
273 1     WCON(5,J),WCON(6,J),WCON(7,J),WCON(8,J),WCON(9,J),
274 1     WCON(10,J),WCON(11,J)
275 59 CONTINUE
276     WRITE(9,109)
277 C
278     WRITE(9,118)EROR
279     WRITE(9,109)
280     IF(T.LE.T1)GO TO 60
281 60     CALL DISPER (RATIO,DISL,DX,DT,DZ)
282 C     -----
283 C
284     SAT=CO
285 C
286     CALL SOLUTE (DX,DZ,DT,TOLER,SAT)
287 C     -----
288 C
289     IF (IFSKIP .EQ. 0) GO TO 62
290     CONTINUE
291     WRITE(9,119)
292     WRITE(9,120)
293     DO 61 J=1,11
294     WRITE(9,117)J,C(1,J),C(2,J),C(3,J),C(4,J),C(5,J),
295 1     C(6,J),C(7,J),C(8,J),C(9,J),C(10,J),C(11,J)
296 61 CONTINUE
297 62 CONTINUE
298 100 FORMAT(E17.8)
299 101 FORMAT(45X,'SOIL TYPE = ',A25)
300 102 FORMAT(42X,'-----')
301 103 FORMAT(10X,'INCREMENTAL LENGTH ALONG X DIRECTION= ',F4.2,' FT')
302 104 FORMAT(10X,'INCREMENTAL LENGTH ALONG Z DIRECTION= ',F4.2,' FT')
303 106 FORMAT(20X,'TIME INCREMENT= ',F8.3)
304 107 FORMAT(20X,'INITIAL MOISTURE CONTENT= ',F6.2)
305 202 FORMAT(20X,'INITIAL SOLUTE CONC. =',F6.1,' mg/L')
306 108 FORMAT(20X,'SOIL POROSITY= ',F5.4)
307 109 FORMAT()
308 110 FORMAT(20X,'TOTAL SIMULATION TIME PERIOD= ',I7,A10)
309 111 FORMAT(20X,'APPLIED TIME PERIOD= ',F6.2,A10)
310 201 FORMAT(20X,'SIMULATION TOLERANCE =',F4.1)

```

```

311 112 FORMAT(30X,'TIME STEP=',I3)
312 113 FORMAT(45X,'      SIMULATION TIME= ',F5.1,A10)
313 114 FORMAT(52X,'-----')
314 115 FORMAT(35X,'      MOISTURE CONTENT AT DIFFERENT NODES')
315 116 FORMAT(37X,'*****')
316 117 FORMAT(5X,I5,11F8.4)
317 118 FORMAT(40X,'ERROR FROM MASS BALANCE=',F12.2,'%')
318 119 FORMAT(30X,'SOLUTE CONCENTRATION AT DIFFERENT NODES: Z-DIRECTION
319 1 ')
320 120 FORMAT(27X,'*****')
321 1*****')
322 *
323 1 CONTINUE
324 CLOSE(9,STATUS='KEEP')
325 STOP
326 END
327 *
328 C
329 C *****
330 C * SUBROUTINE FLOW *
331 C *****
332 C
333 C
334 SUBROUTINE FLOW (DX,DZ,DT,SL,TOLER,SAT)
335 C -----
336 C
337 IMPLICIT REAL*8(A-H,O-Z)
338 DIMENSION SL(11,11)
339 COMMON /PH/ HC(11,11),PHI(11,11)
340 COMMON /COEFF/ E(11,11),F(11,11),D(11,11),H(11,11),B(11,11),
341 1 Q(11,11),QOLD(11,11),QL(11,11),XV(11,11),PNEW(11,11)
342 COMMON /CONST/ M,N,T,T1,JJ
343 DO 301 I=1,M
344 DO 300 J=1,N
345 QOLD(I,J)=0.0
346 QL(I,J)=0.0
347 XV(I,J)=0.0
348 300 CONTINUE
349 301 CONTINUE
350 Z1=DZ**2.
351 Z2=DX**2.
352 Z3=(4.*(DX**2.))
353 Z4=(4.*(DZ**2.))
354 DO 312 I=1,M
355 DO 311 J=1,N
356 J11=J-1
357 J22=J+1
358 I11=I-1
359 I22=I+1
360 IF(I.EQ.1) GO TO 302
361 IF(I.EQ.M) GO TO 303

```

```

362         IF(J.EQ.1) GO TO 304
363         IF(J.EQ.N) GO TO 305
364         D(I,J)=((HC(I,J11)-HC(I,J22))/Z3)+(HC(I,J)/Z2)
365         B(I,J)=((HC(I11,J)-HC(I22,J))/Z4)+(HC(I,J)/Z1)
366         F(I,J)=((HC(I,J22)-HC(I,J11))/Z3)+(HC(I,J)/Z2)
367         H(I,J)=((HC(I22,J)-HC(I11,J))/Z4)+(HC(I,J)/Z1)
368         Q(I,J)=-((HC(I22,J)-HC(I11,J))/(2.*DZ))-(SL(I,J)*PHI(I,J)/DT)
369         GO TO 310
370 302     IF(J.EQ.1) GO TO 306
371         IF(J.EQ.N) GO TO 307
372         D(I,J)=((HC(I,J11)-HC(I,J22))/Z3)+(HC(I,J)/Z2)
373         B(I,J)=0.0
374         F(I,J)=((HC(I,J22)-HC(I,J11))/Z3)+(HC(I,J)/Z2)
375         H(I,J)=2.*HC(I,J)/Z1
376         Q(I,J)=-((HC(I22,J)-HC(I,J))/DZ)-(SL(I,J)*PHI(I,J)/DT)
377         GO TO 310
378 303     IF(J.EQ.1) GO TO 308
379         IF(J.EQ.N) GO TO 309
380         D(I,J)=((HC(I,J11)-HC(I,J22))/Z3)+(HC(I,J)/Z2)
381         B(I,J)=2.*HC(I,J)/Z1
382         F(I,J)=((HC(I,J22)-HC(I,J11))/Z3)+(HC(I,J)/Z2)
383         H(I,J)=0.0
384         Q(I,J)=-((HC(I,J)-HC(I11,J))/DZ)-(SL(I,J)*PHI(I,J)/DT)
385         GO TO 310
386 304     D(I,J)=0.0
387         B(I,J)=((HC(I11,J)-HC(I22,J))/Z4)+(HC(I,J)/Z1)
388         F(I,J)=2.*HC(I,J)/Z1
389         H(I,J)=((HC(I22,J)-HC(I11,J))/Z4)+(HC(I,J)/Z1)
390         Q(I,J)=-(((HC(I22,J)-HC(I11,J))/(2.*DZ))+(SL(I,J)*PHI(I,J)/DT))
391         GO TO 310
392 305     D(I,J)=2.*HC(I,J)/Z2
393         B(I,J)=((HC(I11,J)-HC(I22,J))/Z4)+(HC(I,J)/Z1)
394         F(I,J)=0.0
395         H(I,J)=((HC(I22,J)-HC(I11,J))/Z4)+HC(I,J)/Z1
396         Q(I,J)=-(((HC(I22,J)-HC(I11,J))/(2.*DZ))+(SL(I,J)*PHI(I,J)/DT))
397         GO TO 310
398 306     D(I,J)=0.0
399         B(I,J)=0.0
400         F(I,J)=2.*HC(I,J)/Z2
401         H(I,J)=2.*HC(I,J)/Z1
402         Q(I,J)=-(((HC(I22,J)-HC(I,J))/DZ)+(SL(I,J)*PHI(I,J)/DT))
403         GO TO 310
404 307     D(I,J)=2.*HC(I,J)/Z2
405         B(I,J)=0.0
406         F(I,J)=0.0
407         H(I,J)=2.*HC(I,J)/Z1
408         Q(I,J)=-(((HC(I22,J)-HC(I,J))/DZ)+(SL(I,J)*PHI(I,J)/DT))
409         GO TO 310
410 308     D(I,J)=0.0
411         B(I,J)=2.*HC(I,J)/Z1
412         F(I,J)=2.*HC(I,J)/Z2

```

```

413         H(I,J)=0.0
414         Q(I,J)=-(((HC(I,J)-HC(I11,J))/DZ)+(SL(I,J)*PHI(I,J)/DT))
415         GO TO 310
416 309     D(I,J)=2.*HC(I,J)/Z2
417         B(I,J)=2.*HC(I,J)/Z1
418         F(I,J)=0.0
419         H(I,J)=0.0
420         Q(I,J)=-(((HC(I,J)-HC(I11,J))/DZ)+(SL(I,J)*PHI(I,J)/DT))
421 310     E(I,J)=- (B(I,J)+D(I,J)+F(I,J)+H(I,J)+(SL(I,J)/DT))
422 311     CONTINUE
423 312     CONTINUE
424 C
425         DO 314 I=1,M
426         DO 313 J=1,N
427         PNEW(I,J)=PHI(I,J)
428 313     CONTINUE
429 314     CONTINUE
430 C
431         CALL VECTOR (DX,DZ,TOLER,SAT)
432 C
433 C
434         DO 316 I=1,M
435         DO 315 J=1,N
436         PHI(I,J)=PNEW(I,J)
437 315     CONTINUE
438 316     CONTINUE
439     RETURN
440 END
441 C
442 C
443 C         *****
444 C         * SUBROUTINE VECTOR *
445 C         *****
446 C
447 C         SUBROUTINE VECTOR (DX,DZ,TOLER,SAT)
448 C
449 C         IMPLICIT REAL*8(A-H,O-Z)
450 C         COMMON /COEFF/ E(11,11),F(11,11),D(11,11),H(11,11),B(11,11),
451 1 Q(11,11),QOLD(11,11),QL(11,11),XV(11,11),PNEW(11,11)
452 C         COMMON /PH/ HC(11,11),PHI(11,11)
453 C         COMMON /ACCLP/ K2,KOUNT,W(4)
454 C         COMMON /CONST/ M,N,T,T1,JJ
455 C         ER=0.0
456 C         ITER=0
457 C         KOUNT=0
458 C         K2=4
459 338     ITER=ITER+1
460 C         WRITE(*,336)ITER
461 C         EMAX=0.0
462 C         DO 327 I=1,M
463 C         DO 326 J=1,N

```

```

464         J11=J-1
465         I11=I-1
466         J22=J+1
467         I22=I+1
468         IF(I.EQ.1) GO TO 317
469         IF(I.EQ.M) GO TO 318
470         IF(J.EQ.1) GO TO 319
471         IF(J.EQ.N) GO TO 320
472         QL(I,J)=Q(I,J)-(B(I,J)*PNEW(I11,J))-(D(I,J)*PNEW(I,J11))
473     1 -(E(I,J)*PNEW(I,J))-(F(I,J)*PNEW(I,J22))-(H(I,J)*PNEW(I22,J))
474         GO TO 325
475 317         IF(J.EQ.1) GO TO 321
476         IF(J.EQ.N) GO TO 322
477         QL(I,J)=Q(I,J)-(D(I,J)*PNEW(I,J11))-(E(I,J)*PNEW(I,J))
478     1 -(F(I,J)*PNEW(I,J22))-(H(I,J)*PNEW(I22,J))
479         GO TO 325
480 318         IF(J.EQ.1) GO TO 323
481         IF(J.EQ.N) GO TO 324
482         QL(I,J)=Q(I,J)-(B(I,J)*PNEW(I11,J))-(D(I,J)*PNEW(I,J11))
483     1 -(E(I,J)*PNEW(I,J))-(F(I,J)*PNEW(I,J22))
484         GO TO 325
485 319         QL(I,J)=Q(I,J)-(B(I,J)*PNEW(I11,J))-(E(I,J)*PNEW(I,J))-
486     1 (F(I,J)*PNEW(I,J22))-(H(I,J)*PNEW(I22,J))
487         GO TO 325
488 320         QL(I,J)=Q(I,J)-(B(I,J)*PNEW(I11,J))-(E(I,J)*PNEW(I,J))
489     1 -(D(I,J)*PNEW(I,J11))-(H(I,J)*PNEW(I22,J))
490         GO TO 325
491 321         QL(I,J)=Q(I,J)-(E(I,J)*PNEW(I,J))-(F(I,J)*PNEW(I,J22))-
492     1 (H(I,J)*PNEW(I22,J))
493         GO TO 325
494 322         QL(I,J)=Q(I,J)-(D(I,J)*PNEW(I,J11))-(E(I,J)*PNEW(I,J))
495     1 -(H(I,J)*PNEW(I22,J))
496         GO TO 325
497 323         QL(I,J)=Q(I,J)-(B(I,J)*PNEW(I11,J))-(E(I,J)*PNEW(I,J))
498     1 -(F(I,J)*PNEW(I,J22))
499         GO TO 325
500 324         QL(I,J)=Q(I,J)-(B(I,J)*PNEW(I11,J))-(D(I,J)*PNEW(I,J11))
501     1 -(E(I,J)*PNEW(I,J))
502 325         CONTINUE
503 326         CONTINUE
504 327         CONTINUE
505 C
506         CALL SIP (DX,DZ)
507 C
508 C
509         DO 330 I=1,M
510         DO 329 J=1,N
511             IF (T.GT.T1)GO TO 328
512             IF(I.EQ.1.AND.J.LE.JJ)THEN
513                 PNEW(I,J)=SAT
514             ELSE

```

```

515             PNEW(I,J)=XV(I,J)+PNEW(I,J)
516             ENDIF
517             GO TO 329
518 328             PNEW(I,J)=XV(I,J)+PNEW(I,J)
519 329             CONTINUE
520 330             CONTINUE
521             IF(ITER.EQ.1) GO TO 333
522             DO 332 I=1,M
523                 DO 331 J=1,N
524                     ER=DABS((QOLD(I,J))-(PNEW(I,J)))
525                     IF(ER.GT.EMAX)EMAX=ER
526 331                 CONTINUE
527 332             CONTINUE
528             IF(EMAX.GT.TOLER) GO TO 333
529             GO TO 337
530 333             DO 335 I=1,M
531                 DO 334 J=1,N
532                     QOLD(I,J)=PNEW(I,J)
533 334             CONTINUE
534 335             CONTINUE
535             GO TO 338
536 336             FORMAT(30X,'ITERATION NUMBER=',15)
537 337             RETURN
538             END
539 C
540 C             *****
541 C             * SUBROUTINE DISPER *
542 C             *****
543 C
544             SUBROUTINE DISPER (RATIO,DISL,DX,DT,DZ,)
545 C             -----
546 C
547             IMPLICIT REAL*8(A-H,O-Z)
548             COMMON /PH/ HC(11,11),PHI(11,11)
549             COMMON /SID/ VX(11,11),VZ(11,11),DISX(11,11),DISZ(11,11)
550             COMMON /CONST/ M,N,T,T1,JJ
551 C
552 C             CALCULATION OF TRANSVERSE DISPERSIVITY
553 C             -----
554 C
555             TDIS=RATIO*DISL
556 C
557 C             CALCULATION OF VELOCITY COMPONENT ALONG X AND Z DIRECTIONS
558 C             -----
559 C
560             DO 340 I=1,M
561                 DO 339 J=1,N
562                     J11=J-1
563                     J22=J+1
564                     I11=I-1
565                     I22=I+1

```

```

566         IF(I.EQ.M) THEN
567             VZ(I,J)=HC(I,J)*(PHI(I11,J)-PHI(I,J))/DZ
568         ELSE
569             VZ(I,J)=HC(I,J)*(PHI(I,J)-PHI(I22,J))/DZ
570         ENDIF
571         IF(J.EQ.N) THEN
572             VX(I,J)=(HC(I,J)*(PHI(I,J11)-PHI(I,J))/DX)
573         ELSE
574             VX(I,J)=(HC(I,J)*(PHI(I,J)-PHI(I,J22))/DX)
575         ENDIF
576 C
577 C         CALCULATION OF DISPERSION CO-EFFICIENTS
578 C -----
579 C
580         IF(VX(I,J).EQ.0.0.AND.VZ(I,J).EQ.0.0) THEN
581             DISX(I,J)=0.0
582             DISZ(I,J)=0.0
583         ELSE
584             IF(VZ(I,J).EQ.0.0) THEN
585                 V2=VX(I,J)
586             ELSE
587                 V2=(VX(I,J)/VZ(I,J))**2
588             ENDIF
589             IF(VX(I,J).EQ.0.0) THEN
590                 V3=VZ(I,J)
591             ELSE
592                 V3=(VZ(I,J)/VX(I,J))**2
593             ENDIF
594             V4=(V2/(V2+1))
595             V5=(V3/(V3+1))
596             DISX(I,J)=(DISL*V4)+(TDIS*V5)
597             DISZ(I,J)=(TDIS*V4)+(DISL*V5)
598         ENDIF
599 339         CONTINUE
600 340         CONTINUE
601         RETURN
602     END
603 C
604 C *****
605 C * SUB ROUTINE TO COMPUTE SOLUTE CONCENTRATION AT EACH NODE *
606 C *****
607 C
608         SUBROUTINE SOLUTE (DX,DZ,DT,TOLER,SAT)
609 C -----
610 C
611         IMPLICIT REAL*8(A-H,O-Z)
612         COMMON /COEFF/ E(11,11),F(11,11),D(11,11),H(11,11),B(11,11),
613 1 Q(11,11),QOLD(11,11),QL(11,11),XV(11,11),PNEW(11,11)
614         COMMON /SID/ VX(11,11),VZ(11,11),DISX(11,11),DISZ(11,11)
615         COMMON /CON/ C(11,11)
616         COMMON /ACCLP/ K2,KOUNT,W(4)

```

```

617      COMMON /CONST/ M,N,T,T1,JJ
618          Z1=2.0*(DX**2)
619          Z2=2.0*(DZ**2)
620          Z3=2.0*DX
621          Z4=2.0*DZ
622      A6=1.0/DT
623      DO 451 I=1,M
624          DO 450 J=1,N
625              J11=J-1
626              J22=J+1
627              I11=I-1
628              I22=I+1
629              IF(J.EQ.N) THEN
630                  A2=2.*DISX(I,J)/Z1
631                  A3=2.*VX(I,J)/Z3
632              ELSE
633                  A2=((DISX(I,J22)+DISX(I,J))/Z1)
634                  A3=((VX(I,J22)+VX(I,J))/Z3)
635              END IF
636              IF(I.EQ.M) THEN
637                  A4=2.*DISZ(I,J)/Z2
638                  A5=2.*VZ(I,J)/Z4
639              ELSE
640                  A4=((DISZ(I22,J)+DISZ(I,J))/Z2)
641                  A5=((VZ(I22,J)+VZ(I,J))/Z4)
642              END IF
643              IF(I.EQ.1) GO TO 441
644              IF(I.EQ.M) GO TO 442
645              IF(J.EQ.1) GO TO 443
646              IF(J.EQ.N) GO TO 444
647              D(I,J)=A2+(A3/2.)
648              B(I,J)=A4+(A5/2.)
649              F(I,J)=A2-(A3/2.)
650              H(I,J)=A4-(A5/2.)
651              GO TO 449
652 441      IF(J.EQ.1) GO TO 445
653          IF(J.EQ.N) GO TO 446
654              D(I,J)=A2+(A3/2.)
655              B(I,J)=0.
656              F(I,J)=A2-(A3/2.)
657              H(I,J)=2.*A4
658              GO TO 449
659 442      IF(J.EQ.1) GO TO 447
660          IF(J.EQ.N) GO TO 448
661              D(I,J)=A2+(A3/2.)
662              B(I,J)=2.*A4
663              F(I,J)=A2-(A3/2.)
664              H(I,J)=0.
665              GO TO 449
666 443      D(I,J)=0.
667          B(I,J)=A4+(A5/2.)

```

```

668          F(I,J)=2.*A2
669          H(I,J)=A4-(A5/2.)
670          GO TO 449
671 444      D(I,J)=2.*A2
672          B(I,J)=A4+(A5/2.)
673          F(I,J)=0.
674          H(I,J)=A4-(A5/2.)
675          GO TO 449
676 445      D(I,J)=0.
677          B(I,J)=0.
678          F(I,J)=2.*A2
679          H(I,J)=2.*A4
680          GO TO 449
681 446      D(I,J)=2.*A2
682          B(I,J)=0.
683          F(I,J)=0.
684          H(I,J)=2.*A4
685          GO TO 449
686 447      D(I,J)=0.
687          B(I,J)=2.*A4
688          F(I,J)=2.*A2
689          H(I,J)=0.
690          GO TO 449
691 448      D(I,J)=2.*A2
692          B(I,J)=2.*A4
693          F(I,J)=0.
694          H(I,J)=0.
695 449      E(I,J)=-(B(I,J)+D(I,J)+F(I,J)+H(I,J)+A6)
696          Q(I,J)=-(C(I,J)/DT)
697 450      CONTINUE
698 451      CONTINUE
699          DO 453 I=1,M
700          DO 452 J=1,N
701          PNEW(I,J)=C(I,J)
702 452      CONTINUE
703 453      CONTINUE
704 C
705          CALL VECTOR (DX,DZ,TOLER,SAT)
706 C
707 C
708          DO 455 I=1,M
709          DO 454 J=1,N
710          C(I,J)=PNEW(I,J)
711 454      CONTINUE
712 455      CONTINUE
713      RETURN
714      END
715 C
716 C
717 C          *****
718 C          * SUBROUTINE "SIP" *
719 C          *****

```

```

719 C
720
721 C
722 C
723     IMPLICIT REAL*8(A-H,O-Z)
724     DIMENSION ALPHA(11,11),BETA(11,11),GAMMA(11,11),
725 1     ETA(11,11),DELTA(11,11)
726     COMMON /COEFF/ E(11,11),F(11,11),D(11,11),H(11,11),B(11,11),
727 1     G(11,11),GOLD(11,11),GL(11,11),XV(11,11),PNEW(11,11)
728     COMMON /ACCLP/ K2,KOUNT,W(4)
729     COMMON /CONST/ M,N,T,T1,JJ
730 C
731 C
732 C -----
733 C -COMPUTATION OF CO-EFFICIENTS OF LOWER AND UPPER TRIANGLE -
734 C -      MATRICES BY USING -
735 C -      ALGORITHM DEVELOPED BY REMSON ET.AL, 1971 -
736 C -----
737     KOUNT=KOUNT+1
738     IF(KOUNT.GT.2.AND.K2.EQ.1) GO TO 456
739     IF(KOUNT.GT.2) GO TO 457
740     GO TO 458
741 456     K2=4
742     KOUNT=1
743     GO TO 458
744 457     K2=K2-1
745     KOUNT=1
746 458     CONTINUE
747     AK=W(K2)
748     DO 460 I=1,M
749     DO 459 J=1,N
750     J11=J-1
751     I11=I-1
752     J22=J+1
753     I22=I+1
754     IF(I.EQ.1) THEN
755     C1=0.0
756     ELSE
757     C1=(DELTA(I11,J)*B(I,J))/(1.0+(AK*DELTA(I11,J)))
758     END IF
759     IF(J.EQ.1) THEN
760     G1=0.0
761     ELSE
762     G1=(ETA(I,J11)*D(I,J))/(1.0+(AK*ETA(I,J11)))
763     END IF
764     B1=B(I,J)-AK*C1
765     D1=D(I,J)-AK*G1
766     E1=E(I,J)+AK*C1+AK*G1
767     F1=F(I,J)-AK*C1
768     H1=H(I,J)-AK*G1
769     ALPHA(I,J)=B1

```

```

770         BETA(I,J)=D1
771         IF(J.EQ.1)THEN
772             IF(I.EQ.1)THEN
773                 GAMMA(I,J)=E1
774             ELSE
775                 GAMMA(I,J)=E1-(ETA(I11,J)*ALPHA(I,J))
776             END IF
777         ELSE
778             IF(I.EQ.1) THEN
779                 GAMMA(I,J)=E1-(BETA(I,J)*DELTA(I,J11))
780             ELSE
781                 GAMMA(I,J)=E1-(ALPHA(I,J)*ETA(I11,J))-(BETA(I,J)*DELTA(I,J11))
782             ENDIF
783         END IF
784         DELTA(I,J)=F1/GAMMA(I,J)
785         ETA(I,J)=H1/GAMMA(I,J)
786 459     CONTINUE
787 460     CONTINUE
788 C
789 C
790 C     - SOLVE FOR UNKNOWNNS (PHI(I,J) OR C(I,J)) BY FORWARD-
791 C     - AND BACKWARD SUBSTITUTION.
792 C
793 C
794 C         FORWARD SUBSTITUTION
795 C
796 C
797         DO 466 I=1,M
798             DO 465 J=1,N
799                 J11=J-1
800                 I11=I-1
801                 IF(J.GT.1) GO TO 462
802                 IF(I.GT.1) GO TO 461
803                 XV(I,J)=QL(I,J)/GAMMA(I,J)
804                 GO TO 464
805 461             XV(I,J)=(QL(I,J)-(XV(I11,J)*ALPHA(I,J)))/GAMMA(I,J)
806                 GO TO 464
807 462             IF(I.EQ.1) GO TO 463
808                 XV(I,J)=(QL(I,J)-(BETA(I,J)*XV(I,J11))-(ALPHA(I,J)*
809 1                 XV(I11,J)))/GAMMA(I,J)
810                 GO TO 464
811 463             XV(I,J)=(QL(I,J)-(BETA(I,J)*XV(I,J11)))/GAMMA(I,J)
812 464             CONTINUE
813 465             CONTINUE
814 466             CONTINUE
815 C     BACKWARD SUBSTITUTION IN UPPER TRIANGULAR MATRIX
816         DO 472 I=M,1,-1
817             DO 471 J=N,1,-1
818                 J22=J+1
819                 I22=I+1
820                 IF(J.LT.N) GO TO 468

```

```

821             IF(I.LT.M) GO TO 467
822             XV(I,J)=XV(I,J)
823             GO TO 470
824 467        XV(I,J)=XV(I,J)-(ETA(I,J)*XV(I22,J))
825             GO TO 470
826 468        IF(I.EQ.M) GO TO 469
827             XV(I,J)=XV(I,J)-(ETA(I,J)*XV(I22,J))-(DELTA(I,J)*XV(I,J22))
828             GO TO 470
829 469        XV(I,J)=XV(I,J)-(DELTA(I,J)*XV(I,J22))
830 470        CONTINUE
831 471        CONTINUE
832 472        CONTINUE
833             RETURN
834 END
835 C
836 C
837 C             *****
838 C             * SUBROUTINE INTPOL *
839 C             *****
840             SUBROUTINE INTPOL (PRES,THETA,SL,P,FMC,KK,SATP)
841 C             -----
842 C
843             IMPLICIT REAL*8(A-H,O-Z)
844             DIMENSION PRES(11,11),THETA(11,11),SL(11,11),P(21),FMC(21)
845             COMMON /CONST/ M,N,T,T1,JJ
846 C             P(LK)= HYDROSTATIC PRESSURE DATA FROM THE TABLE
847 C             FMC(LK)= MOISTURE CONTENT VALUES FROM THE TABLE
848 C             LK= NUMBER OF DATA POINTS IN THE TABLE
849 C
850 C             LOCATE POSITION OF PRES(I,J) IN TABLE P(KK)
851 C             -----
852 C
853             DO 487 I=1,M
854             DO 486 J=1,N
855             IF(PRES(I,J).LT.P(1).OR.PRES(I,J).GT.P(KK)) GO TO 488
856             IF(PRES(I,J).LT.SATP) GO TO 473
857             L3=KK-1
858             GO TO 483
859 473        L1=1
860             L2=KK
861             L3=(L1+L2)/2
862 474        IF(P(L3).LE.PRES(I,J).AND.P(L3+1).GT.PRES(I,J)) GO TO 475
863             IF(P(L3).LE.PRES(I,J)) L1=L3
864             IF(P(L3).GT.PRES(I,J)) L2=L3
865             L3=(L1+L2)/2
866             GO TO 474
867 C
868 C             SOLVE FOR THETA(I,J) AND SL(I,J)
869 C             -----
870 C
871 C             SOLVE FOR THETA(I,J) WHEN J3=1

```

```

872 C
873 C
874 475      IF(L3.GT.1) GO TO 476
875          A=DLOG(DABS(FMC(3)/FMC(2)))/DLOG(DABS(P(3)/P(2)))
876          B=DLOG(DABS(FMC(3)))-A*DLOG(DABS(P(3)))
877          RLOG1=A*DLOG(DABS(PRES(I,J)))+B
878          RH2=DLOG(DABS(P(1)))*A+B
879          IF(RLOG1.LT.RH2) RLOG1=RH2
880          THETA(I,J)=10.**RLOG1
881          SL(I,J)=A*THETA(I,J)/PRES(I,J)
882          GO TO 485
883 476      IF (L3.GT.3) GO TO 478
884          S1=(FMC(2)-FMC(1))/(P(2)-P(1))
885          S2=(FMC(3)-FMC(2))/(P(3)-P(2))
886          S3=(FMC(4)-FMC(3))/(P(4)-P(3))
887          IF (L3.EQ.3) GO TO 477
888          T2=(DABS(S3-S2)*S1+DABS(S2-S1)*S2)/(DABS(S3-S2)+DABS(S2-S1))
889          T5=(S1+S2)/2.
890          GO TO 484
891 477      S4=(FMC(5)-FMC(4))/(P(5)-P(4))
892          T2=(DABS(S4-S3)*S2+DABS(S2-S1)*S3)/(DABS(S4-S3)+DABS(S2-S1))
893          T5=(DABS(S3-S2)*S1+DABS(S2-S1)*S2)/(DABS(S3-S2)+DABS(S2-S1))
894          GO TO 484
895 478      IF (L3.GE.KK-2) GO TO 482
896          S1=(FMC(L3-1)-FMC(L3-2))/(P(L3-1)-P(L3-2))
897          S2=(FMC(L3)-FMC(L3-1))/(P(L3)-P(L3-1))
898          S3=(FMC(L3+1)-FMC(L3))/(P(L3+1)-P(L3))
899          S4=(FMC(L3+2)-FMC(L3+1))/(P(L3+2)-P(L3+1))
900          S5=(FMC(L3+3)-FMC(L3+2))/(P(L3+3)-P(L3+2))
901          IF(S5.NE.S4.AND.S3.NE.S2) GO TO 479
902          T2=(S4+S3)/2.0
903          GO TO 480
904 479      T2=(DABS(S5-S4)*S3+DABS(S3-S2)*S4)/(DABS(S5-S4)+DABS(S3-S2))
905 480      CONTINUE
906          IF(S4.NE.S3.AND.S2.NE.S1) GO TO 481
907          T5=(S3+S2)/2.0
908          GO TO 484
909 481      T5=(DABS(S4-S3)*S2+DABS(S2-S1)*S3)/(DABS(S4-S3)+DABS(S2-S1))
910          GO TO 484
911 482      IF (L3.GT.KK-2) GO TO 483
912          S1=(FMC(KK-3)-FMC(KK-4))/(P(KK-3)-P(KK-4))
913          S2=(FMC(KK-2)-FMC(KK-3))/(P(KK-2)-P(KK-3))
914          S3=(FMC(KK-1)-FMC(KK-2))/(P(KK-1)-P(KK-2))
915          S4=(FMC(KK)-FMC(KK-1))/(P(KK)-P(KK-1))
916          T2=(DABS(S4-S3)*S2+DABS(S3-S2)*S4)/(DABS(S4-S3)+DABS(S3-S2))
917          T5=(DABS(S4-S3)*S2+DABS(S2-S1)*S3)/(DABS(S4-S3)+DABS(S2-S1))
918          GO TO 484
919 483      S2=(FMC(KK-2)-FMC(KK-3))/(P(KK-2)-P(KK-3))
920          S3=(FMC(KK-1)-FMC(KK-2))/(P(KK-1)-P(KK-2))
921          S4=(FMC(KK)-FMC(KK-1))/(P(KK)-P(KK-1))
922          T2=(S4+S3)/2.0

```

```

923      T5=(DABS(S4-S3)*S2+DABS(S3-S2)*S4)/(DABS(S4-S3)+DABS(S3-S2))
924 484      CONTINUE
925      R1=P(L3+1)-P(L3)
926      R2=(3.0*(FMC(L3+1)-FMC(L3))/R1-2.0*T5-T2)/R1
927      R1=(T5+T2-2.0*(FMC(L3+1)-FMC(L3))/R1)/(R1**2)
928      RV2=PRES(I,J)-P(L3)
929      THETA(I,J)=FMC(L3)+T5*RV2+R2*RV2**2+R1*RV2**3
930      SL(I,J)=T5+2.*R2*RV2+3.*R1*RV2**2
931      RAD=4.0*R2**2-12.0*T5*R1
932      IF(RAD.LT.0) GO TO 485
933      THETA(I,J)=FMC(L3)+(PRES(I,J)-P(L3))*(FMC(L3+1)-FMC(L3))/
934 1      (P(L3+1)-P(L3))
935      SL(I,J)=(FMC(L3+1)-FMC(L3))/(P(L3+1)-P(L3))
936 485      CONTINUE
937 486      CONTINUE
938 487      CONTINUE
939      GO TO 489
940 488      WRITE(9,490)PRES(I,J),I,J
941      STOP
942 489      CONTINUE
943 490      FORMAT('PRESSURE OR PERMEABILITY VALUE IS OUT OF RANGE',5X,
944 1      E17.8,3X,2I4)
945      RETURN
946      END
947 C
948 C      *****
949 C      * SUBROUTINE "MASS" *
950 C      *****
951 C
952      SUBROUTINE MASS (VOL,EROR)
953 C      -----
954 C
955      IMPLICIT REAL*8(A-H,O-Z)
956      COMMON /MBAL/ WW,SLWC(1,11)
957      COMMON /WATER/ WCON(11,11)
958      COMMON /CONST/ M,N,T,T1,JJ
959      WV=0.
960      IF(T.GT.T1) GO TO 492
961      DO 491 J=1,JJ-1
962      J22=J+1
963      WC1=(WCON(1,J)+WCON(2,J)+WCON(1,J22)+WCON(2,J22))/4.
964      WW=WW+((WC1-WCON(2,J))*VOL/2.)
965 491      CONTINUE
966 492      DO 494 I=1,M-1
967      DO 493 J=1,N-1
968      I22=I+1
969      J22=J+1
970      WC1=(WCON(I,J)+WCON(I22,J)+WCON(I,J22)+WCON(I22,J22))/4.
971      WV=WV+(VOL*WC1)
972 493      CONTINUE
973 494      CONTINUE

```

```
974      EROR=DABS((MW-WV)/MW)*100
975      RETURN
976  END
```

APPENDIX B

**Soil characteristic data for
three soil types**

AMARILLO SILT CLAY

H.C. (IN/HR)	PRES (FEET)	Percent Saturation (DECIMAL)
2.05E-37	-4095.8006	0.0
4.549EE-35	-1860.3536	0.05
3.81E-33	-1419.0311	0.10
3.192E-31	-1082.4075	0.15
2.674E-29	-825.6356	0.20
2.24E-27	-629.7762	0.25
1.876E-25	-480.3759	0.30
1.572E-23	-372.6181	0.35
1.317E-21	-309.536	0.40
3.125E-19	-278.3645	0.45
2.688E-18	-257.3084	0.50
6.042E-18	-240.997	0.55
9.912E-18	-226.3052	0.60
1.524E-17	-213.9992	0.65
2.51E-17	-202.9942	0.70
4.124E-17	-192.1329	0.75
6.133E-17	-180.8873	0.80
8.542E-17	-169.3132	0.85
1.177E-16	-150.4948	0.90
1.58E-16	-100.3097	0.95
2.05E-16	-65.5328	1.00

POUDAR RIVER SAND

H.C. (IN/HR)	PRES (FEET)	Percent Saturation (DECIMAL)
0	-2056.32	0.0
0	-324.076	0.05
0	-204.4106	0.10
0	-141.4551	0.15
0	-115.3474	0.20
8.014E-22	-102.3019	0.25
2.885E-16	-93.6363	0.30
1.038E-10	-86.24145	0.35
1.1E-05	-81.20408	0.40
1.996E-05	-77.45911	0.45
4.1E-04	-74.47901	0.50
6.993E-05	-71.82376	0.55
1.127E-04	-69.38682	0.60
1.884E-04	-67.24372	0.65
3.024E-04	-65.49043	0.70
4.650E-04	-64.73296	0.75
6.888E-04	-64.4718	0.80
1.061E-03	-63.72536	0.85
1.348E-03	-62.04497	0.90
1.635E-03	-56.92799	0.95
1.734E-03	-41.94893	1.00

FINE SAND

H.C. (IN/HR)	PRES (FEET)	Percent Saturation (DECIMAL)
0	-3314.86	0.0
2.462E-18	-881.1488	0.05
1.309E-14	-511.8337	0.10
6.918E-11	-297.3081	0.15
4.667E-07	-169.9124	0.20
1.284E-04	-119.9345	0.25
1.404E-03	-102.8230	0.30
5.581E-03	-94.19022	0.35
1.381E-02	-88.64056	0.40
3.333E-02	-84.63246	0.45
6.566E-02	-81.39515	0.50
.10885	-78.62031	0.55
.17563	-76.1538	0.60
.28984	-73.99559	0.65
.48635	-71.68323	0.70
.88640	-68.9084	0.75
1.5261	-65.51693	0.80
1.8804	-61.663	0.85
2.1668	-56.5758	0.90
2.345	-49.48456	0.95
2.345	-1.5416E-06	1.00

APPENDIX C

**Test data collected from the
groundwater tracer test**

BROMIDE CONCENTRATION ANALYSIS DATA

DAYS AFTER INJECTION	A	B	C	D	E	F	G	H	J	K
-18.0	3.70	3.70	3.18	4.05	3.50	3.55	3.70	2.50	3.70	2.50
-15.0	1.01	0.92	3.20	4.05	3.50	3.05	3.70	2.71	3.70	2.71
-9.0	2.50	12.59	6.10	4.90	3.50	2.50	3.01	2.36	3.10	1.80
-8.0	2.20	18.87	7.80	5.60	3.55	3.30	3.70	2.51	3.70	2.60
-7.0	2.80	19.60	8.70	8.40	3.01					
-6.0	4.50	25.90	7.43	7.40	3.50					
-5.0	3.50	27.61	5.51	6.43	3.28					
-1.0	1.67	X	2.85	2.42	2.44	3.01	3.69	2.75	2.11	4.19
0.0	1.36	X	2.66	2.39	2.01	2.77	2.32	2.58	1.25	4.55
1.0	3.18	3640.00	4.54	3.41	2.95	2.90	2.27	2.72	4.54	4.99
1.5		3840.00								
2.0		3940.00								
2.5		3549.00								
3.0	3.50	3394.00	5.01	5.00	3.50	2.53	2.50	3.41	4.45	4.50
3.5		2748.00								
5.0	4.00	3815.00	3.80	6.00	4.01	3.10	3.20	3.50	4.50	4.55
7.0	3.42	2700.00	4.05	7.60	4.50	3.60	4.01	4.50	4.05	4.55
9.0	4.05	1592.00	3.66	8.50	3.81	3.66	5.33	5.50	4.05	4.56
11.0	4.01	976.00	5.60	9.76	4.45	6.71	7.30	4.55	3.80	4.10
12.0	3.60	802.80	6.30	12.20	5.83	9.37	10.25	3.90	3.53	3.50
13.0	3.96	912.60	8.10	25.40	6.08	12.15	13.50	3.50	4.10	3.47
14.0	2.40	1083.60	8.60	38.72	13.10	8.27	15.91	8.31	4.71	4.05
17.0	2.63	1068.00	9.30	40.58	19.00	8.10	22.40	19.48	3.91	4.10
18.0	1.32	1457.00	9.80	45.24	24.72	7.38	25.23	24.99	4.01	4.30
19.0	2.63	1481.00	10.13	28.67	26.85	8.30	37.35	28.67	4.30	4.10
21.0	3.24	555.10	10.52	42.21	39.04	9.20	51.73	49.30	4.05	3.91
24.0	6.84	599.60	12.40	45.50	47.60	9.45	54.70	52.86	4.82	4.05
26.0	2.40	758.00	14.31	46.77	56.54	11.55	58.90	58.01	3.19	4.10
28.0	3.95	159.80	13.80	42.94	58.32	10.73	67.10	59.29	3.40	4.05
31.0	3.50	104.20	14.52	43.39	67.87	11.01	67.87	65.45	3.81	4.05
33.0	3.05	108.00	14.08	48.87	66.69	11.50	83.70	77.22	3.23	4.05
35.0	4.05	105.00	10.80	49.95	76.68	10.50	84.78	72.09	3.82	4.10
38.0	3.66	161.93	10.96	48.77	84.67	11.41	98.91	76.17	4.30	4.13
40.0	4.05	96.66	5.40	42.39	86.40	12.31	115.02	72.90	4.80	3.90
42.0	4.05	92.61	5.40	44.01	88.83	13.01	135.00	86.67	5.92	4.55
45.0	4.05	84.24	4.05	46.44	90.18	14.32	152.00	86.67	6.37	4.83
47.0	4.01	75.29	9.35	38.18	88.11	14.00	169.60	91.05	6.20	5.50
49.0	4.05	189.80	10.68	46.99	100.93	13.71	175.20	97.46	7.83	5.55
52.0	6.25	72.00	10.00	43.25	78.75	12.63	173.80	82.00	7.10	5.50
54.0	6.25	47.00	6.25	37.00	94.50	10.54	162.50	96.25	7.23	6.10
56.0	3.75	49.40	6.25	38.25	99.75	10.32	146.00	100.00	6.49	6.10
60.0	6.10	40.26	6.10	39.28	95.16	10.01	139.30	86.13	8.01	6.23
62.0	5.60	98.00	5.60	40.60	98.28	9.51	139.40	87.92	8.45	7.86
64.0	5.60	57.96	5.60	32.76	106.40	9.32	129.10	87.90	8.10	5.91
69.0	6.70	55.80	6.70	28.30	91.05	12.00	86.24	78.23	9.21	6.43
71.0	5.90	53.90	5.70	22.00	107.80	8.17	92.40	109.70	8.01	7.72
74.0	5.70	50.05	4.77	18.50	107.80	6.81	102.40	109.34	8.35	8.17
78.0	5.60	54.29	5.40	11.53	86.63	6.58	91.63	120.10	7.50	6.81
82.0	4.75	37.31	5.60	11.38	96.46	10.01	53.24	94.50	6.55	6.58
85.0	4.05	36.86	5.05	10.01	96.92	11.83	53.69	73.81	4.50	7.13
89.0	4.01	30.02	5.55	8.55	92.80	10.10	40.48	59.90	8.01	6.23
96.0	3.75	32.39	5.05	9.41	105.80	8.30	22.34	47.06	7.05	7.12
100.0	3.75	35.28	5.60	8.23	94.08	6.91	15.30	42.35	7.06	7.05

BROMIDE CONCENTRATION ANALYSIS DATA

DAYS AFTER INJECTION	A	B	C	D	E	F	G	H	J	K
104.0	3.66	19.80	4.81	3.96	88.35	7.10	9.53	48.67	4.03	4.95
107.0	4.01	27.90	4.55	3.10	119.35	7.38	18.60	58.90	5.89	3.72
114.0	3.10	29.76	4.55	7.75	125.55	8.27	19.84	68.82	6.82	4.65
118.0	3.72	26.40	4.71	6.93	125.40	7.10	18.49	72.60	10.56	9.90
123.0	4.10	19.47	4.83	6.60	112.20	7.10	15.18	73.26	2.59	9.24
126.0	7.07	29.29	7.10	8.10	111.10	7.10	18.20	80.80	10.10	14.14
130.0	8.08	20.20	8.10	8.10	121.20	7.10	17.17	80.80	6.06	13.13
132.0	8.08	25.25	7.07	7.10	111.10	8.10	7.07	70.70	8.10	12.12
140.0	7.05	13.60	4.21	6.73	110.00	4.21	6.05	87.50	6.41	12.50
143.0	5.49	13.10	2.83	4.81	103.10	4.50	6.10	85.30	4.02	10.81
150.0	3.20	9.80	2.51	4.50	91.30	3.20	3.50	90.20	3.51	6.71
153.0	3.41	8.41	2.24	4.51	85.40	2.10	3.10	79.80	3.30	8.24
160.0	5.50	5.43	3.05	4.20	80.20	2.10	2.81	85.30	2.50	5.33
168.0	3.20	4.08	3.01	4.30	75.00	2.50	2.50	92.50	2.50	4.05
176.0		2.50		3.23	35.10		1.60	45.90	1.87	3.00
185.0		1.76		2.30	34.40		1.70	41.58	1.70	2.53
190.0		1.90		1.90	27.00		1.90	40.50	1.80	1.90
197.0	1.63	1.80	1.80	1.80	48.60	1.90	1.80	75.60	1.80	1.90
213.0	1.66	1.60	1.65	1.60	40.02	1.73	1.65	82.25	2.01	1.65
218.0	1.60	1.60	1.60	1.60	25.94	1.65	1.60	70.10	1.65	1.65
226.0	1.60	1.60	1.60	1.60	24.84	1.66	1.60	66.24	1.66	1.60
251.0	1.83	1.80	2.10	1.60	15.60	2.10	1.80	69.60	2.31	2.10
265.0	1.80	1.80	2.23	2.10	18.00	2.20	2.10	74.40	2.40	2.10
278.0	2.00	1.80	2.30	2.30	22.20	2.50	2.30	78.00	2.80	2.10
295.0	3.81	3.81	3.49	3.05	11.78	3.17	2.79	52.07	4.57	3.81
297.0	2.50	2.10	1.90	2.23	12.95	2.06	2.21	50.80	3.10	2.21

APPENDIX D

**Sample input file used in the
USGS-2D model program**

